Quantum Electronics **35** (12) 1085 – 1103 (2005)

REVIEW

PACS numbers: 42.81. – i; 42.79.Dj
DOI: 10.1070/QE2005v035n12ABEH013041

Fibre gratings and their applications

S.A. Vasil'ev, O.I. Medvedkov, I.G. Korolev, A.S. Bozhkov, A.S. Kurkov, E.M. Dianov

***Abstract*. A brief review is given of the state of the art in the research on the photosensitivity of fibres and photoinduced fibre gratings. The most important properties of fibre gratings are considered and the main methods of their production and their applications are discussed. The photosensitive compositions of silica glasses are presented and methods for increasing their photosensitivity are indicated.**

Keywords: *optical fibre, fibre Bragg grating, refractive index, long-period grating.*

1. Introduction

The photorefractivity of a doped silica glass, i.e., the ability to change its refractive index under the action of radiation is being now actively studied and finds wide applications in fibreoptic communication systems, fibre lasers, systems for measuring various physical quantities, etc. Processes occurring in glasses exposed to radiation are often described in the scientific literature by using a broader concept of 'photosensitivity', meaning that not only the refractive index of the glass changes upon its irradiation but also a number of its other material properties. A few thousands of scientific papers have been already published in this field, the International Conferences (Bragg Gratings, Photosensitivity, and Poling in Glass Fibres and Waveguides: Applications and Fundamentals, BGPP) and Scientific Schools for Young Scientists (Summer School on Photosensitivity in Optical Waveguides and Glasses, POWAG) are being held, and topical journals [1] and monographs [2, 3] have been published.

The formation of permanent gratings in fibres was first discovered in 1978 [4]. The authors of this paper coupled radiation from a single-frequency argon laser into the core of a germanosilicate fibre. Within a few minutes after the beginning of irradiation, they observed strong reflection of radiation caused by some modification of fibre properties. The authors explained this effect by the appearance of a standing wave in the fibre due to Fresnel reflection of light from its opposite end. The refractive index of the fibre changes in the maxima of this wave, resulting in the formation of a grating reflecting radiation according to the Bragg condition and amplifying it during irradiation. It was shown later that a variation (increase) in the refractive index induced by visible light is a two-photon process [5], and the writing of fibre Bragg gratings (FBGs) by UV radiation through the side surface of a germanosilicate fibre was proposed in 1989; in this case, one-photon excitation into the absorption band of a germanosilicate glass was used [6]. It is the latter publication, which opened up the possibility of changing the spectral parameters of gratings within a broad range and demonstrated the real outlook for practical applications of fibre gratings, that stimulated active studies in the field of development of photoinduced structures in fibres.

In this review, we describe the most important properties and characteristics of the main types of photoinduced fibre gratings, present the basic methods for fibre grating production and radiation sources used for this purpose, consider the photosensitive compositions of glasses and photosensitivity types in germanosilicate fibres, and also discuss the most important applications of FBGs.

2. The main types of fibre gratings

Fibre grating is a region of an optical fibre (as a rule, single-mode) with a periodic structure of the refractive index with the period Λ induced in the fibre core, which has a certain spatial distribution shown schematically in Fig. 1. As a rule, the grating is produced in photosensitive core (*1*) of the fibre, whereas the refractive index of silica cladding (*2*) remains unchanged. Such a structure has unique spectral characteristics, which determine its wide applications in a

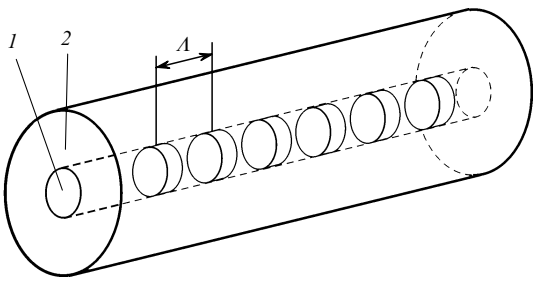

Figure 1. Scheme of a fibre refractive-index grating: (*1*) photosensitive fibre core; (*2*) silica cladding.

S.A. Vasil'ev, O.I. Medvedkov, I.G. Korolev, A.S. Bozhkov, A.S. Kurkov, E.M. Dianov Fiber Optics Research Center, A.M. Prokhorov General Physics Institute, Russian Academy of Sciences, ul. Vavilova 38, 119991 Moscow, Russia; e-mail: sav@fo.gpi.ru, ivan@fo.gpr.ru

Received 19 September 2005
Kvantovaya Elektronika **35** (12) 1085 – 1103 (2005)
Translated by M.N. Sapozhnikov

variety of devices in fibre optics. For example, the most important property of FBGs is narrowband reflection of optical radiation with a relative spectral width of 10^{-6} and smaller.

The advantages of photoinduced fibre gratings over alternative reflectors (for example, interference mirrors and bulky diffraction gratings) are obvious: these are a variety of spectral and dispersion characteristics, many of which can be obtained only in fibre gratings, all-fibre design, low optical losses, a comparatively simple fabrication, etc.

An electromagnetic wave propagating along a fibre can be represented as a combination of the guided and radiation modes of the fibre. Guided modes are characterised by a set of propagation constants β_i, whereas radiation modes form a continuum of β. In the absence of perturbations of the wave field in the fibre, these modes propagate not interacting with each other.

The fibre grating structure is fabricated to provide the required resonance interaction between the specified modes of the fibre. Note that the theory of resonance interactions on periodic structures is developed in detail, is widely used in various fields of physics and is applicable in most cases to the description of the properties of fibre gratings. The interaction of the fibre modes is usually described by the theory of coupled modes [7], which assumes that only two modes satisfy the phase-matching condition at a certain wavelength and, therefore, can efficiently transfer energy to each other. It is also assumed that the mode fields in the presence of a weak periodic perturbation remain invariable. These conditions are fulfilled in most cases considered below.

Two modes interact on a homogeneous fibre grating, i.e., on the structure in which the refractive index periodically changes with a constant period Λ if the phase-matching condition

$$\beta_2 - \beta_1 = \frac{2\pi N}{\Lambda} \tag{1}$$

is fulfilled, where β_1 and β_2 are the propagation constants of the modes under study; and N is an integer characterising the order in which the intermode interaction occurs. The mode propagation constant is described by the relation $\beta_i = 2\pi n_{\text{eff}}^i/\lambda$, where n_{eff}^i is the effective refractive index of the ith mode; and λ is the wavelength in vacuum.

Consider the interaction of the fundamental HE_{11} (LP_{01}) mode of a fibre with other guided and radiation modes. Figure 2 shows different types of the intermode coupling for $N = 1$ [8]. On the vertical axis the effective refractive index of the fibre modes is plotted (n_{co}, n_{cl}, and n_{ext} are the refractive indices of the fibre core, cladding, and environment, respectively). The positive and negative directions of the vertical axis characterise the fibre modes propagating forward and backward with respect to the initial fundamental HE_{11} mode, respectively. Figure 2 presents the dispersion curves for the core ($n_{\text{cl}} < n_{\text{eff}} < n_{\text{co}}$) and cladding ($n_{\text{ext}} < n_{\text{eff}} < n_{\text{cl}}$) modes. The hatched region corresponds to radiation modes. Dashed curves (*1*) and (*2*) denote the values $n_{\text{eff}}^{\text{co}} - \lambda/\Lambda$ for gratings with small ($\Lambda_{\text{BG}} \leqslant 1$ μm, FBGs) and large [$\Lambda_{\text{LPG}} \geqslant 100$ μm, long-period fibre gratings (LPFG)] periods, where $n_{\text{eff}}^{\text{co}}$ is the effective refractive index for the fundamental mode.

The intersection points of these curves with the dispersion curves of different modes specify the wavelengths at which phase-matching condition (1) is satisfied. Note that

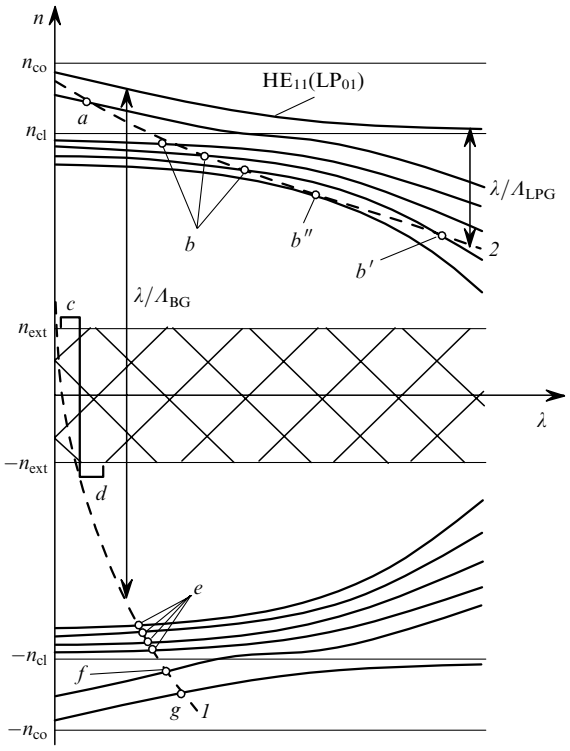

Figure 2. Diagram demonstrating the fulfilment of phase-matching condition between the fundamental HE_{11} (LP_{01}) mode and other modes of the fibre.

for large periods Λ, the coupling with modes propagating in the same direction appears in the grating, whereas for small periods Λ, the coupling occurs with counterpropagating modes. Figure 2 clearly illustrates the coupling between the fundamental mode of the fibre core with different core (*a*, *f*, *g*) and cladding (*b*, *e*) modes and radiation modes (*c*, *d*) propagating in the forward (*a*–*c*) and backward (*d*–*g*) directions.

Note that the same grating at different wavelengths can couple the fundamental core mode with modes of different types and different propagation directions. Thus, the spectra of FBGs with the high reflectance usually exhibit resonances to the blue with respect to the main reflection band, which are related to excitation of cladding modes [9] (points *e* in Fig. 2). As a rule, the resonance coupling with the higher-order cladding modes in LPFG spectra is realised at longer wavelengths [10] (*b*). At the same time, for certain parameters of the fibre and grating, the inverse intersection of the above dispersion dependences can occur (point *b′*), resulting in the additional resonance interaction with the same cladding mode. Note that the spectral sensitivity of such a peak to external perturbations has the opposite sign compared to the 'usual' resonance peak [11]. A special case of resonance interaction on a LPFG is a contact of the dispersion curves under study (point *b″*), which is characterised by a considerable broadening of the LPFG absorption peak and by the fact that the external perturbations are manifested in this case not in the shift of the resonance wavelength but in the change of the peak depth [11].

Apart from the types of fibre gratings described above, there also exist the so-called mode and polarisation converters, which are less common gratings but also have a number of interesting applications. Mode converters [12]

written in few-mode fibres convert radiation from one core mode to another (points *a* and *f* in Fig. 2). A similar process is realised in polarisation converters, where the interaction of the modes with mutually perpendicular polarisations of the electric field is performed on a grating written in a birefringent optical fibre [13, 14].

3. Fibre Bragg gratings

Fibre Bragg gratings couple the fundamental mode of an optical fibre with the same mode propagating in the opposite direction. This means that radiation propagating in the fibre at a certain wavelength $\lambda_{BG} = 2n_{eff}^{co}\Lambda_{BG}$ is reflected from the grating according to (1) completely or partially. The characteristics of this reflection depend on the grating parameters. For a homogeneous grating of length L, the reflectance R at the resonance wavelength λ_{BG} is described by the expression $R = \tanh^2(\kappa_{BG}L)$, where $\kappa_{BG} = \pi\Delta n_{mod}\eta_{BG}/\lambda_{BG}$ is the coupling coefficient; Δn_{mod} is the index modulation amplitude in the first order of the pitch-profile expansion into the Fourier series;

$$\eta_{BG} = \int_0^a |E_{co}|^2 r\mathrm{d}r \Big/ \int_0^\infty |E_{co}|^2 r\mathrm{d}r$$

is the power fraction of the fundamental mode propagating in the fibre core of radius a; and E_{co} is the electric field amplitude of the fundamental mode.

The spectral width of the resonance of a homogeneous FBG measured between the first zeroes of its reflection spectrum is described by the expression

$$\Delta\lambda_{BG,0} = 2\lambda_{BG}\frac{\Lambda_{BG}}{L}\left[1 + \left(\frac{\kappa_{BG}L}{\pi}\right)^2\right]^{1/2}. \qquad (2)$$

One can see from (2) that for gratings with a low reflectance ($\kappa_{BG}L \ll \pi$) the relative spectral width $\Delta\lambda/\lambda$ depends only on the number of pitches in the grating $N_{BG} = L/\Lambda_{BG}$. At the same time, as $\kappa_{BG}L$ increases, the spectral width of the resonance increases and becomes proportional to the coupling coefficient for $\kappa_{BG}L \gg \pi$. The spectral properties of the FBG are illustrated in Fig. 3 by the wavelength dependences of the reflectance R and the group delay τ calculated for gratings of length $L = 5$ mm for $\kappa_{BG}L = 0.38$ and 5.7.

The reflection spectra presented in Fig. 3 were calculated for the same grating period chosen so that the resonance wavelength λ_{BG} for the unperturbed core was 1500.0 nm. During FBG writing, its resonance wavelength shifts to the red due to an increase in the average refractive index n_{eff} upon exposing the fibre to UV light. This shift depends on the contrast of the interference pattern and does not exceed, as a rule, 1 nm (Fig. 3).

The reflection spectra of homogeneous gratings, both FBGs and LPFG, exhibit usually side maxima (Fig. 3) whose position is determined by the grating length. To suppress these maxima partially or completely, the so-called grating apodization is used, i.e., a slow variation in the modulation amplitude of the induced refractive index along the grating length [15]. Thus, the use of a Gaussian envelope of the induced index profile in a FBG (Fig. 4) provides the elimination of side maxima to the red from the main resonance. The presence of side maxima on the blue side is caused by a change in the average induced refractive index $\Delta n_{avr}(z)$ in the grating; they can be eliminated by providing the constant value of this index over the entire grating length (see Fig. 5) [16].

The temporal dispersion of light pulses in modern fibreoptic communication links can be compensated by means of gratings with the resonance wavelength changing

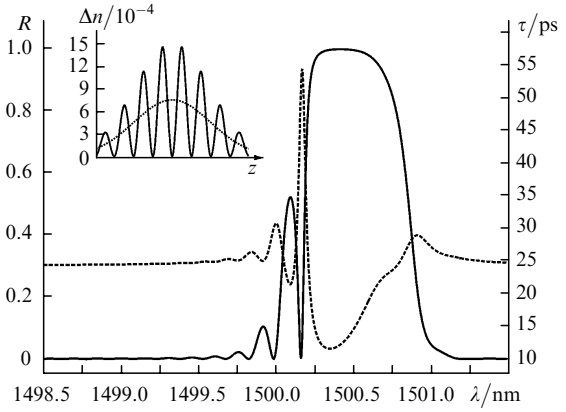

Figure 4. Reflection spectrum $R(\lambda)$ (solid curve) and group delay $\tau(\lambda)$ (dashed curve) for a FBG with the Gaussian envelope of the induced refractive-index profile.

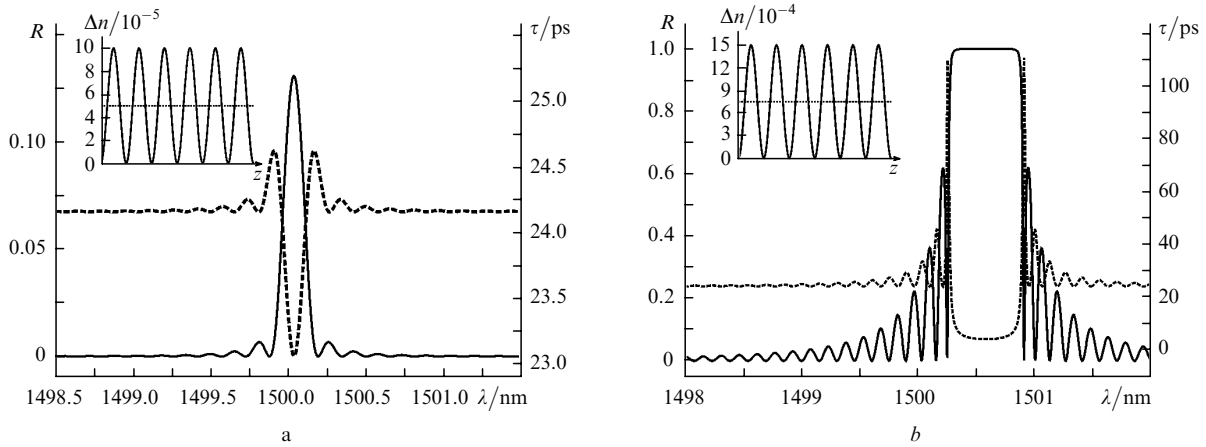

Figure 3. Reflection spectrum $R(\lambda)$ (solid curve) and group delay $\tau(\lambda)$ (dashed curve) of uniform FBGs for $\kappa_{BG}L = 0.38$ (a) and 5.7 (b). Inserts show the refractive-index profile induced in gratings.

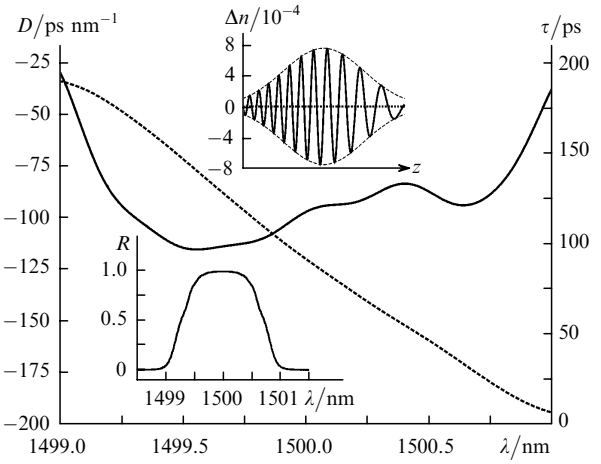

Figure 5. Dispersion $D(\lambda)$ (solid curve) and group delay $\tau(\lambda)$ (dashed curve) of a FBG with the Gaussian envelope of the induced refractive-index profile and a variable period. Inserts show the reflection spectrum $R(\lambda)$ of the grating and the schematic profile of the induced refractive index $\Delta n(z)$.

continuously [17] or stepwise [18] along their length in a specified way. Such chirped gratings have a broad reflection (transmission) spectrum (broader than 100 nm [19]) or large dispersion (more than 1000 ps nm^{-1} [20]). The gratings of this type are written by changing the modulation period of the induced refractive index [21] or effective index of the fundamental mode [22] over the fibre length. Figure 5 illustrates the calculated spectral characteristics of a FBG with a variable period, corresponding to a 1 nm cm^{-1} linear variation in the resonance wavelength, and a Gaussian profile of the envelope of the index modulation amplitude at a constant average refractive index.

In the literature, several special FBG structures are considered [2, 3, 16]. The most important of them are:

(i) Phase-shifted Bragg gratings. The introduced phase shift leads to the appearance of a narrow transmission band of width of a few tens of megahertz within the reflection band. Figure 6 shows the calculated transmission spectrum of such a grating. The phase shift in the grating can be introduced during the writing of the whole structure [23] or later in the preliminary written grating [24]. As the phase shift is increased (which is usually realised by writing two spatially separated gratings with the same λ_{BG}), the number of transmission regions in the reflection band increases, and such a structure is called, similarly to bulk optics, a Fabry–Perot interferometer (or filter).

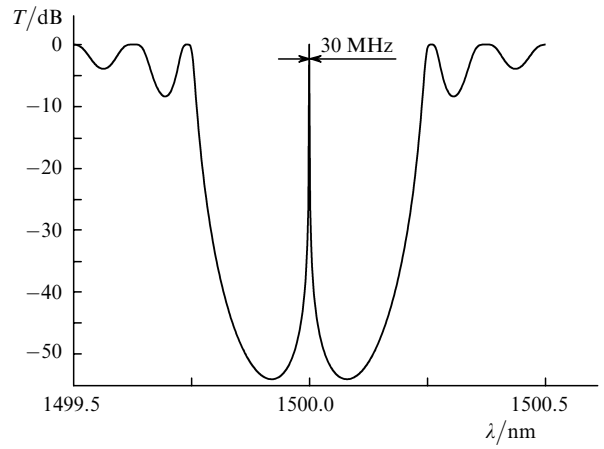

Figure 6. Transmission spectrum of a FBG of length 10 mm with the phase shift π in the middle.

(ii) Superstructured (sampled) Bragg gratings [25, 26]. If the FBG parameters vary periodically over the grating length with a period that greatly exceeds the grating period (usually 0.1 – 10 mm), several narrow peaks appear in the grating spectrum, which cover a certain spectral interval. Such superstructured FBGs are fabricated, as a rule, by a successive writing of separate periodically arranged FBGs.

(iii) Superimposed Bragg gratings [27]. Several successively superimposed gratings with different periods can be written in the same region of the core of a highly photosensitive fibre. Although the superposition of each successive grating reduces the reflectance of the previous gratings, nevertheless the writing of a superposition of seven FBGs with the reflectance 50 % – 60 % was demonstrated [27].

(iii) Tilted (blazed) Bragg gratings [28]. The tilt of the FBG fringe plane with respect to the fibre axis enhances the coupling of the fundamental mode of the fibre with cladding modes or radiation modes. Such gratings can be used to fabricate nonreflecting fibre filters of different widths, which can be also employed to modify the gain and luminescence spectra of broadband radiation sources [28].

(iv) Multimode fibre Bragg gratings [29]. The possibility of FBG writing in several types of standard multimode or few-mode fibres was considered in paper [29], where it was shown, in particular, that the reflection spectrum of a FBG in a multimode graded-index fibre consists of approximately 20 spectrally resolved peaks corresponding to the resonances of different modes and located at a wavelength of $\sim$1550 nm within the region of width $\sim$10 nm. Obviously, the spectrum of multimode FBGs strongly depends on the mode composition of radiation propagating in the fibre, which opens up the possibility to analyse the degree of excitation of one or the other of guided modes.

The resonance wavelength λ_{BG} of a FBG depends on the fibre temperature and mechanical tensile or compressive stresses applied to the fibre. This dependences is described by the equation [30]

$$\delta\lambda_{BG} = 2n_{eff}^{co}\Lambda_{BG}\left\{\left\{1 - \frac{(n_{eff}^{co})^2}{2}\left[P_{12} - \nu(P_{11} + P_{12})\right]\right\}\varepsilon + \left[\alpha + \frac{1}{n_{eff}^{co}}\frac{dn_{eff}^{co}}{dT}\right]\delta T\right\}, \quad (3)$$

where δT is the temperature change; ε is the applied mechanical stress; P_{ij} are the Pockels coefficients of the elastooptic tensor; ν is the Poisson coefficient; α is the thermal expansion coefficient of silica glass. This relation gives the typical temperature shift of $\sim$0.01 nm K^{-1} and the shift of λ_{BG} depending on the relative elongation of the fibre $\sim 10^3 \times \delta L L^{-1}$ nm.

4. Long-period fibre gratings

Photoinduced long-period fibre gratings were first proposed in paper [31]. Gratings of this type have a relatively large period $\Lambda_{LPG} = 100 - 500$ μm and couple a mode of the fibre core with cladding modes propagating in the same direction. As a rule, cladding modes are guided by the silica

glass–air interface, which is formed after removing a protective jacket from the irradiated region of the fibre. The energy transferred to a cladding mode is then absorbed in a protective jacket covering the fibre, resulting in the appearance of the absorption band at the resonance wavelength in the transmission spectrum of the fibre, which, according to (1), is described by the expression

$$\lambda_{\mathrm{LPG}} = \left(n_{\mathrm{eff}}^{\mathrm{co}} - n_{\mathrm{eff}}^{\mathrm{cl}}\right)\Lambda_{\mathrm{LPG}} = \Delta n_{\mathrm{eff}}\Lambda_{\mathrm{LPG}}. \quad (4)$$

The cladding of a standard fibre (of diameter 125 μm) can support many modes ($\sim 10^4$). However, only few modes (namely, HE_{1m} and EH_{1n}, where m and n are the radial mode numbers) have the large overlap integral with the core mode field taken over the region where the index modulation is induced (for photoinduced gratings, this region is the germanosilicate core of the fibre):

$$\eta_{\mathrm{LPG}} = \int_0^a E_{\mathrm{co}}E_{\mathrm{cl}}^* r\mathrm{d}r \Big/ \left(\int_0^\infty |E_{\mathrm{co}}|^2 r\mathrm{d}r \int_0^\infty |E_{\mathrm{cl}}|^2 r\mathrm{d}r\right)^{1/2}, \quad (5)$$

where E_{cl} is the electric-field amplitude of the corresponding cladding mode. Such modes have the axial symmetry and the number of oscillations along the fibre radius equal to the radial mode number [32]. Note that cladding modes excited in a LPFG are numbered in many papers in the order of decreasing their propagation constant [9]. In this notation, the HE_{1m} modes have an odd number p, while the EH_{1n} modes have an even number, and the relations $p = 2(m-1) - 1$ and $p = 2n$ are valid. The overlap integral for the HE_{1m} modes increases with increasing m up to $m \leqslant 10$ and decreases, by oscillating, as the radial mode number further increases. The value of η_{LPG} for the EH_{1n} modes increases for small n significantly slower [9], so that, as a rule, absorption resonances related to the HE_{1m} modes of the order $m \leqslant 20$ dominate in the LPFG spectra.

Unlike a FBG, the absorption peak depth in a LPFG is the oscillating function $S = \sin^2(\kappa_{\mathrm{LPG}}L)$, where κ_{LPG} is the coupling coefficient, which, as in the case of a FBG, is described by the relation $\kappa_{\mathrm{LPG}} = \pi\Delta n_{\mathrm{mod}}\eta_{\mathrm{LPG}}/\lambda_{\mathrm{LPG}}$, where λ_{LPG} is the resonance wavelength of the LPFG. For $\kappa_{\mathrm{LPG}}L = \pi/2$, energy at the wavelength λ_{LPG} completely transfers from the core mode to the corresponding cladding mode, so that LPFGs with $\kappa_{\mathrm{LPG}}L \leqslant \pi/2$ are most often used for practical purposes.

The full spectral width of the LPFG peak in the region of the first oscillation $\kappa_{\mathrm{LPG}}L \leqslant \pi$ measured by the first zeroes of the reflectance is described by the expression

$$\Delta\lambda_{\mathrm{LPG},0} = 2\alpha_{\mathrm{BRF}}\lambda_{\mathrm{LPG}}\frac{\Lambda_{\mathrm{LPG}}}{L}\left[1 - \left(\frac{\kappa_{\mathrm{LPG}}L}{\pi}\right)^2\right]^{1/2}, \quad (6)$$

where α_{BRF} is bandwidth refinement factor, which can be larger or smaller than unity [33]. This additional factor takes into account the spectral dependence $\Delta n_{\mathrm{eff}}(\lambda)$.

The specific features of a LPFG are illustrated in Fig. 7, where the transmission spectrum of the grating of length 10 mm and period 122 μm is presented. The spectrum was calculated for a step-index fibre (the core-cladding index difference was $\Delta n = 0.02$) with the cladding diameter 80 μm and the cut-off wavelength for the first higher mode $\lambda_{\mathrm{c}} = 0.9$ μm. The induced refractive index was taken to be 5×10^{-4} in calculations.

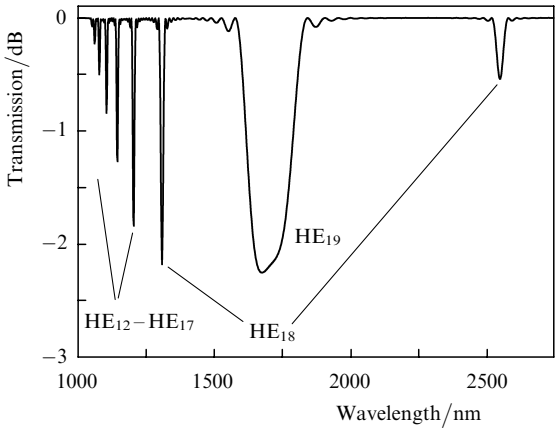

Figure 7. Transmission spectrum of a uniform LPFG (grating parameters are presented in the text).

This spectrum corresponds to the situation shown schematically in Fig. 2 [curve (*2*)]. The spectral region $\lambda < 1500$ nm is typical for a LPFG: in this region the intensity of intermode interaction monotonically increases with increasing the radial mode number m of the cladding HE_{1m} modes. Note also the specific features of the LPFG discussed in the analysis of Fig. 2, namely, the presence of the second, weaker resonance for the HE_{18} mode in the long-wavelength region and a considerable broadening of the coupling peak with the HE_{19} mode.

The spectral characteristics of a LPFG depend on the fibre temperature, tension, and bending, as well as on the refractive index of the fibre environment [34, 35]. These questions were recently studied in detail experimentally and theoretically in paper [11].

The influence of temperature T on the LPFG spectrum is mainly manifested in the shift of the resonance wavelength λ_{LPG}. The temperature sensitivity $\delta\lambda_{\mathrm{LPG}}/\delta T$ of the resonance wavelength of the LPFG depends on the number of a coupled cladding mode and is typically 0.05–0.1 nm K^{-1}. The temperature sensitivity of the grating is described by the expression [34]

$$\frac{\delta\lambda_{\mathrm{LPG}}}{\lambda_{\mathrm{LPG}}} = \delta T\left[\frac{1}{\Delta n_{\mathrm{eff}}}\frac{\partial(\Delta n_{\mathrm{eff}})}{\partial T} + \frac{1}{\Lambda_{\mathrm{LPG}}}\frac{\partial\Lambda_{\mathrm{LPG}}}{\partial T}\right] \times\left[1 - \Lambda_{\mathrm{LPG}}\frac{\partial(\Delta n_{\mathrm{eff}})}{\partial\lambda}\right]^{-1}. \quad (7)$$

The second term in the numerator of this equation, which is the thermal expansion coefficient of silica glass, can be neglected, as a rule, compared to the first term. Therefore, the main factors determining the temperature sensitivity of a LPFG are the thermooptic coefficients of the fibre core and cladding, as well as the spectral dependences of the effective refractive indices of coupled modes at the wavelength under study [the second term in the denominator in (7)]. Note that it is the decrease in the dominator with increasing the cladding mode number that enhances the temperature sensitivity of the LPFG peaks observed in experiments [11, 34].

The tensile sensitivity of LPFGs was studied in papers [11, 35, 36]. It was found that, depending on the fibre type, the absorption peak sensitivity can vary within a broad range from 15 to −7 nm per 1 % of the relative elongation of

the grating [35]. The value and sign of this coefficient are determined by the difference of the elastooptic coefficients of the fibre core and cladding [11].

The sensitivity $\delta\lambda_{LPG}/\delta n_{ext}$ of the resonance wavelength to variation in the external refractive index of the environment can achieve $\sim 10^4$ nm if this refractive index is slightly lower than the refractive index of the silica cladding of the fibre. When $n_{ext} > n_{cl}$, the resonance wavelength becomes insensitive to the refractive index n_{ext} of the environment [37].

The transmission spectrum of a LPFG is highly sensitive to the fibre bending. On the one hand, this requires a very careful fixation of the grating in a setup, and on the other makes these gratings promising for using as bending and deformation sensors. Spectral variations caused by fibre bending depend on the fibre geometry, the refractive index profile, the profile of elastic stresses, and some other factors. As a rule, they are revealed in a decrease in the depth of the resonance peak and its shift to the red [38]. In addition, new resonance peaks appear due to the interaction with the EH_{1n} modes. Changes in the LPFG spectra caused by the fibre bending are so strong that the fibre bending with a curvature of ~ 1 m can be quite easily detected. If a fibre has no axial symmetry or asymmetry is produced in some way during LPFG writing or after it, a change in the grating spectrum depends on the bending direction [39, 40].

The propagation constant of cladding modes depends on the fibre cladding diameter. This fact makes it possible to perform rather easily the irreversible shift of the resonance wavelength of the grating [41]. The cladding diameter can be decreased, for example, by fibre etching in the solution of hydrofluoric acid HF. This procedure allows one to shift the resonance wavelength by a rather large distance without changing, in fact, the coupling coefficient of the grating. The wavelength shift increases with increasing the cladding mode number, and can achieve 100 nm and more for high-order modes [41].

As in the case of a FBG, the side maxima in the LPFG spectra are suppressed by using apodization of the induced index profile [42, 43]. The LPFG writing was demonstrated with a period variable along the fibre length [42, 44] and with the phase shift in the grating structure [45]. Because of a relatively large period of such gratings, the required profile of a grating pitch can be produced, which can exclude, for example, the excitation of higher-order resonances [42, 43]. Finally, two spatially separated LPFGs can be used to form a Mach–Zehnder interferometer, whose optical arms are the core and cladding modes in the space between the gratings [46]. Such an interferometer, having a high temperature stability, provides, for example, the measurement of the induced refractive index in the fibre core with an accuracy better than 10^{-6} [47].

5. Methods for fibre grating fabrication

Photoinduced fibre gratings are written, as a rule, by exposing a fibre to intense UV light (see Section 6).

Because the FBG period is small ($\Lambda \sim 0.5$ μm), FBGs are usually produced by interferometric methods. Since the FBG writing process can last for a few tens of minutes, a high-quality grating can be fabricated only when the interference pattern is very stable. Although the number of methods proposed for FBG writing is quite large [2, 3], their main features can be distinguished.

In the first interferometer used for FBG writing [6] (Fig. 8a), an incident UV beam was split into two beams with a beamsplitter, which were subsequently recombined at the fibre at an angle of α to each other. This angle determines the period of an interference pattern and, hence, the FBG period.

FBGs are often written by using interferometers with a spatially split beam, which have a smaller number of optical elements and, therefore, a better stability. Such an interferometer can use, for example, a dielectric mirror, which splits the beam front into two equal parts (a Lloyd interferometer in Fig. 8b). The angle α is varied in this case by rotating the mirror together with the fibre fixed on it, which is much simpler than the angle tuning used in the interferometer shown in Fig. 8a. Note that a cylindrical lens in both schemes in Fig. 8 is used to focus radiation on the fibre (in some cases, on its core), which is necessary, as a rule, for increasing the UV radiation density to write the FBG. Interferometers of these types allow a flexible variation of grating parameters such as their period and length; however, they require the high spatial and time coherence of writing radiation.

The phase-mask technique for FBG writing proposed in [48] (Fig. 9a) does not require highly coherent UV radiation, and therefore inexpensive excimer lasers can be used in this case. This method utilises interference between the first and minus first diffraction orders of radiation passed through a phase mask. The mask is made, as a rule, of silica glass

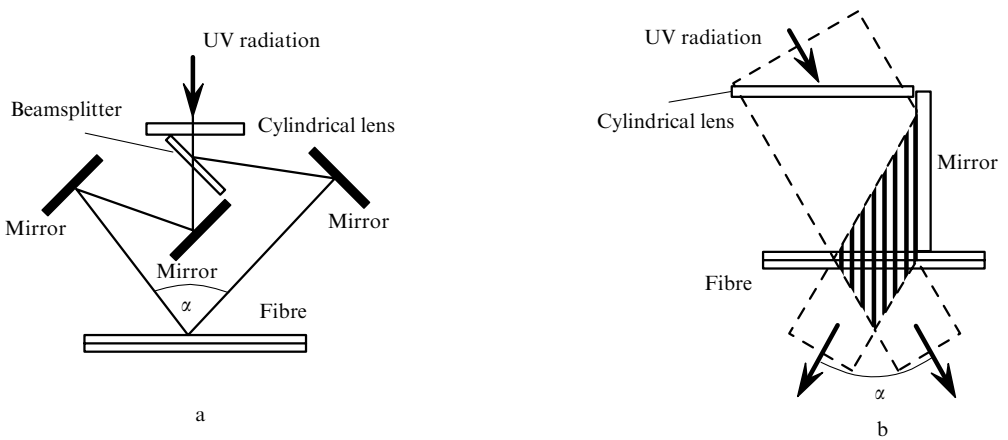

Figure 8. Schemes of FBG writing in interferometers with the amplitude (a) and spatial (b) splitting of a UV radiation beam.

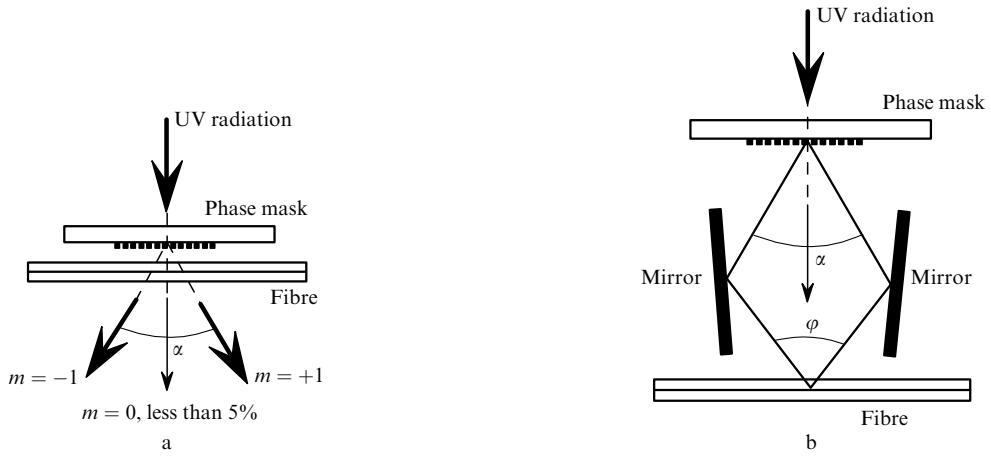

Figure 9. Schemes of FBG writing by the phase-mask method: direct writing (a) and writing in a Talbot interferometer (b).

transparent in the UV spectral region. The relief of its surface facing the fibre is fabricated so that to suppress the zero and other diffraction orders (except the first ones), thereby providing a high contrast of the interference pattern. Note that the use of phase masks allows the production of FBGs with the modulation period and amplitude variable along the fibre length. However, the primary disadvantage of this technique is a rigid fixation of the possible FBG parameters at the stage of mask fabrication. In the phase-mask method, the resonance wavelength of the FBG can be tuned in a relatively broad range by rotating additional mirrors in a Talbot interferometer [49] (Fig. 9b).

Note also that gratings with an arbitrary distribution of the induced refractive index can be fabricated by the mask-scanning technique [50, 51]. This method can be used to produce complex grating structures with the modulation period and amplitude, and average refractive index varying along the fibre length.

The fabrication of gratings directly during fibre drawing has become an independent and quite important direction of studies [52, 53]. This method enables the production of a series of FBGs with different λ_{BG} immediately before applying a protective coating on the fibre. Each of the gratings of the chain is written by one pulse from an excimer laser. The resonance wavelength is tuned before FBG writing by tuning the interferometer (Fig. 8a). This writing method allows the increase in the mechanical strength of the fibre grating section and production of many gratings in certain regions of the fibre. Although such FBG series are quite attractive for distributed measurements of various physical quantities, the complexity of the writing system and the insufficient stability of its parameters prevent wide applications of this method in practice.

Methods for LPFG fabrication differ considerably from FBG writing methods because the typical periods of former gratings are two-three magnitudes greater, which considerably alleviates the requirements to the mechanical stability of the writing system and coherence of UV radiation. The most widespread LPFG writing methods are the amplitude mask method [54] and the step-by-step method [55].

Upon LPFG writing through the amplitude mask (Fig. 10a), all the grating structure is formed simultaneously, as a rule, and grating writing as a whole takes the same time as the writing of an individual grating pitch. When pulsed sources are used, this method is most preferable because the pulse energy density cannot be considerably increased due to a relatively low damage threshold of the silica glass surface (~ 1 J cm^{-2} for excimer laser radiation).

In the step-by-step method (Fig. 10b), the required periodic grating structure is produced successively by displacing the fibre mechanically with respect to the laser beam focused on the fibre core. In this method, it is preferable to use cw lasers because in this case the UV radiation density can be increased and, hence, the LPFG writing time is reduced. The step-by-step writing method is more flexible because it enables the production of arbitrary profiles of individual grating pitches and the entire amplitude distribution of the induced refractive index and the variation of the grating period along the grating length.

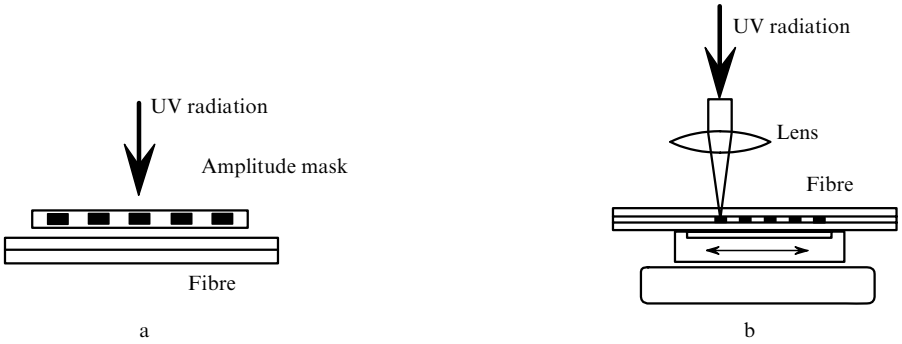

Figure 10. LPFG writing by UV radiation with the help of an amplitude mask (a) and by the step-by-step method (b).

LPFGs can be also fabricated by the step-by-step method by using the local heating of the fibre up to high temperatures (above 1000 °C). Such thermal action can change the index profile for a number of reasons: the mechanical deformation of the fibre [56], the redistribution of the existing elastic stresses [57, 58], and the spatial redistribution of the chemical composition of glass due to the thermal diffusion of dopants in the fibre core [59, 60]. The thermal action can be produced by IR lasers (CO_2 laser [61], CO laser [62]) or by a localised electric discharge [63, 64].

Sufficiently deep thermally induced gratings (i.e., with a sufficiently large coupling coefficient) can be written in non-photosensitive or low-photosensitive fibres, for example, in fibres with a pure silica core [58]. Because gratings are induced upon the local heating of the fibre up to the temperature close to the melting temperature of silica glass, they have a higher thermal stability compared to photo-induced gratings and are not damaged even at temperatures of the order of 1000 °C [62]. At the same time, thermally induced gratings, as a rule, introduce spectrally independent ('grey') losses caused by the mechanical deformation of the fibre during LPFG writing. Because the rate of thermally induced processes strongly depends on temperature, uniform gratings can be obtained only in the case of a high reproducibility of the heating temperature and the thermal exposure time from step to step. This reproducibility is usually insufficient, resulting in the inhomogeneity of the spectrum observed in the most above-mentioned papers. In addition, because of thermal transfer along the fibre axis, the region of thermal action is, as a rule, of the order of the fibre diameter, which complicates the writing of small-period gratings ($\Lambda \leqslant 200$ μm).

LPFGs can be also fabricated by periodic deformation [65] or etching [66] of the fibre.

Apart from the irreversible LPFG writing, there exist methods for reversible grating fabrication in fibres. In [67], a LPFG was produced by a travelling acoustic wave at frequency ~2 MHz. In this case, the coupling efficiency and the resonance wavelength are specified by the amplitude and frequency of the high-frequency signal, respectively, whereas the length of the fibre region with a polymer coating removed determines the grating length and, consequently, the spectral width of the resonance. A specific feature of such a grating is the possibility to control flexibly its spectral characteristics and to produce simultaneously several LPFGs by applying simulteneously several radio-frequency signals.

Note in the conclusion of this section that the number of papers devoted to the LPFG production in prospective microstructure fibres [68–71], in which FBG writing is complicated [72], has increased.

6. UV sources used for grating writing

Mechanisms of photoinduced variations in the refractive index in silica glass are still not finally clear even for the most studied glasses doped with germanium dioxide. However, it is known that photoexcitation of germanium oxygen-deficient centres (GODCs) [73] in a germanosilicate glass initiates the subsequent transformation of the glass network, which is accompanied by a change in its refractive index. The absorption spectrum of a germanosilicate glass exhibits the two bands at 242 and 330 nm, which are assigned to the singlet–singlet and singlet–triplet absorption by GODCs, respectively. Optical excitation into the singlet band can be performed by a KrF excimer laser at 248 nm, the second harmonics of an argon laser at 244 and 257 nm, the fourth harmonic of a Nd^{3+}:YAG laser at 266 nm, and the second harmonic of dye lasers. These lasers are used, as a rule, to write fibre gratings.

The triplet absorption band is weaker by three orders of magnitude [73]; however, as follows from [55, 74], it can be also used to induce noticeable index variations ($\sim 2 \times 10^{-4}$). A comparative analysis of index variations produced upon singlet and triplet excitation of GODCs showed that the dominant mechanism of these variations is the transformation of these centres from the excited triplet state irrespective of the band used for excitation [47]. The advantage of excitation into the triplet absorption band is that the grating can be written in this case without removing a protective polymer jacket from the fibre, which is partially transparent in this spectral range [75].

Note that radiation of ArF and F_2 excimer lasers at 193 nm [76] and 157 nm [77], respectively, also induces considerable variations in the refractive index of silica glasses, and not only germanosilicate glasses.

Depending on the fibre photosensitivity and a laser used, the UV dose required for fibre writing varies from 1 to 100 kJ cm^{-2}. This corresponds, taking the radiation density into account, to the exposure time from a few seconds to a few tens of minutes.

Currently the number of papers devoted to the use of femtosecond laser pulses for grating writing [78, 79] has increased. Because of a very high radiation intensity ($\sim 10^{13}$ W cm^{-2}) produced in such short pulses, multi-photon radiation absorption takes place in this case. Such a mechanism of the index variation does not require the fibre doping with photosensitive dopants and hydrogen loading (see Section 7). The 800-nm femtosecond pulses from a Ti:sapphire laser were used to write high-quality FBGs with a large induced refractive index (10^{-2}) by the phase-mask method in standard SMF-28 fibres [78] and in fibres with a pure silica core [80]. Such gratings can be written in any region of a fibre, by producing the required index distributions along the fibre cross section. For example, this circumstance was used in [81] to form a periodic structure in the fibre core, which provided a considerable decrease in the coupling coefficient of the fundamental mode of the fibre with cladding modes. Fibre gratings written by femtosecond pulses have a very high thermal stability (above 1000 °C). Because the writing wavelength is comparatively long, such FBGs are written, as a rule, with a period corresponding to the second or third diffraction order [$N = 2$, 3 in Eqn (1)].

7. Photosensitive glass compositions and methods for photosensitivity increasing

The value of the refractive index induced in the fibre core depends on many factors such as the method and conditions of the fibre fabrication, the type and concentration of dopants, the wavelength, intensity and type of irradiation (pulsed or continuous).

Unfortunately, the photosensitivity of standard telecommunication fibres with the molar concentration of GeO_2 equal to 3 %–5 % is not high enough for the efficient writing of gratings in them. The refractive index variation

induced in such fibres does not exceed 5×10^{-5} even after a long exposure. For this reason, considerable efforts have been devoted to the search for the methods to increase the photosensitivity. It was shown, in particular, that the photosensitivity of germanosilicate fibres increases with increasing concentration of germanium dioxide in the fibre core [82], which is explained by the increase in the GODC concentration with increasing the degree of doping of glasses with germanium. Absorption at 242 nm is usually proportional to the molar concentration of GeO_2 with the proportionality coefficient $10-40$ dB (mm %)$^{-1}$ [83]. By now fibres with different concentrations of germanium dioxide have been studied. It was shown, in particular, that, beginning from the molar concentration of GeO_2 equal to 20 %, the photosensitivity of type IIa appears in the fibre (see Section 8), which is preserved and enhanced with further increasing GeO_2 concentration [84]. The photosensitivity of type IIa is also observed in nitrogen-doped fibres irradiated at 193 nm [85]. Note that gratings of type IIa are rarely used in practice because fibres with such a photosensitivity have high intrinsic losses and high losses in splices with standard fibres.

A noticeable increase in the GODC concentration can be also achieved by synthesising a fibre preform under the oxygen deficiency conditions, for example, by replacing oxygen by nitrogen or noble gases [86], which enables the enhancement of the core glass photosensitivity by preserving the waveguide properties of the fibre almost invariable [87].

Among the chemical elements enhancing the photosensitivity of fibres upon co-doping with germanium are boron [88, 89], tin [90], nitrogen [91], phosphorous [92], and antimony [93].

Fibres not containing GeO_2, in which the index profile was formed by other dopants, were studied in a number of papers. Thus, it was found that fibres doped with nitrogen [85], phosphorous [94, 95], sulphur [96], and antimony [97] had a high photosensitivity upon irradiation at a wavelength of 193 nm.

Although a number of fibre compositions having a high photosensitivity have been proposed, such fibres are difficult to fabricate, as a rule, and their material and waveguide characteristics differ from the standard ones. The latter circumstance often leads to additional losses in splices with standard fibres and to some other complications in the use of such fibres.

In this connection it was interesting to attempt to increase the photosensitivity of already fabricated fibres, in particular, standard fibres not varying considerably their intrinsic characteristics. It was found that the hydrogen loading of a glass network at high temperatures, for example, in a burner flame with a high content of hydrogen can increase the induced refractive index in standard fibres by an order of magnitude [98]. Such loading, which can be performed in a small region of the fibre, provides the enhanced sensitivity in this region for a long time. At the same time, it leads to a considerable absorption caused by the appearance of the OH groups, and also reduces the mechanical strength of fibres.

In [99], an essentially different method of hydrogen loading was proposed, which also significantly enhances the photosensitivity of germanosilicate fibres and is now most often used in practice. The glass network is loaded with molecular hydrogen at relatively low temperatures (no more than 100 °C). At such temperatures, molecular hydrogen does not yet interact with the glass network and is physically dissolved in the glass. Such loading is performed by immersing a fibre into a chamber containing hydrogen at a pressure of ~ 100 atm. The diffusion coefficient of molecular hydrogen in a silica glass is rather high and exponentially depends on temperature [100],

$$D_{H_2} = 2.83 \times 10^{-4} \exp \frac{-40.19(\text{kJ mol}^{-1})}{RT} \text{ cm}^2 \text{ s}^{-1}$$

(where R is the gas constant), so that almost complete loading of a standard fibre (98 % of the maximum value) at room temperature is achieved after two weeks and at a temperature of 100 °C already after 12 hours. The molar concentration of H_2 in the glass network after such processing achieves $2\,\%-3\,\%$ [100]. Fibres loaded with hydrogen at low temperatures have the enhanced photosensitivity until hydrogen is contained in the glass. During the out diffusion of hydrogen to the environment, the photosensitivity decreases, returning to its initial value, so that the hydrogen-loaded fibre should be kept at low temperature. Thus, at $T = -20$ °C the hydrogen concentration at the fibre axis decreases by half approximately after two months.

The above-described method of hydrogen loading is most convenient in practice and provides the refractive-index induction in standard fibres at a level of $\sim 10^{-2}$ [99], which is sufficient for most applications. However, this method has a number of disadvantages. In particular, the thermal stability of gratings written in a hydrogen-loaded fibre proves to be comparatively low [101], which requires the additional annealing of gratings before their use. Also, it should be taken into account that hydrogen dissolved in the glass changes its refractive index, resulting in a shift of the resonance wavelength of the grating [102]. The value of this shift depends on the initial hydrogen concentration and can achieve a few nanometres for FBGs [103] and a few tens of nanometres for LPFGs [104].

Apart from these complications inherent in hydrogen-loaded fibre gratings, note that UV irradiation causes the formation of OH groups absorbing in the IR spectral region. This absorption at a wavelength of 1.4 μm can achieve a few dB cm^{-1} [105]. To avoid this absorption, deuterium is used instead of hydrogen, whose absorption bands are strongly shifted to the red due to its larger atomic mass [106].

The useful development of the low-temperature hydrogen-loading technique was proposed in [107], where it was shown that, by exposing a hydrogen-loaded fibre to low-intense UV light, it is possible to 'freeze' the high photosensitivity of the fibre, i.e., to preserve it for a long time even after the escape of molecular hydrogen from the fibre. In this way, it is possible to prepare the required regions of the fibre for subsequent grating writing by irradiating them preliminary. It was found that such preliminary processing can be performed not only at the writing wavelength but also at other UV wavelengths, in particular, by radiation from a UV lamp.

An interesting effect was observed in [108], where it was shown that the mechanical stretching of a fibre during grating writing results in a considerable increase in its photosensitivity. The authors observed the three-fourfold increase in the induced refractive index at fixed irradiation

parameters compared to the unstretched fibre, which allows one to decrease the grating writing time by an order of magnitude. The disadvantage of this method for increasing photosensitivity is the necessity of producing rather strong deformations (3% and more), which requires the high quality of the fibre surface and the mechanical stability of the stretching system during grating production. In addition, such stretching deformations considerably change the resonance wavelength of the grating, which should be taken into account for obtaining the required resonance wavelength in the fibre without mechanical loading.

8. Photosensitivity types in germanosilicate fibres

Physical phenomena taking place during the exposure of a germanosilicate glass to UV radiation are rather numerous. However, the experimental facts available at present cannot be described within the framework of a unitary model. The matter is that variations in the refractive index of a silica glass are determined simultaneously by several mechanisms, which complicates the analysis and interpretation of the experimental data. At the same time, it is known that the photoinduced transformation of GODCs accompanied by the formation of new defect centres [109, 110] and the glass-network rearrangement makes a considerable contribution to the variation in the refractive index in the core of germanosilicate fibres. The glass-network rearrangement results in an increase in the glass density [111, 112], a change in its Raman spectrum [113], and is accompanied by an increase in elastic stresses in the fibre core [114].

At present several types of photosensitivity of germanosilicate fibres are known. They are manifested under different exposure conditions and differ from each other in the writing and annealing dynamics, and in some other properties of photoinduced gratings.

Type I gratings. If the molar concentration of GeO_2 in the core of a fibre is lower than 20 % (as, for example, in standard telecommunication fibres), the so-called type I photosensitivity is realised, which is characterised by a monotonic increase in the refractive index with increasing the UV dose [115] [curve (*1*) in Fig. 11]. This type of photosensitivity is characterised by the power dependence $\Delta n_{ind} \sim D^b$ of the induced refractive index on the dose, the exponent b being, as a rule, in the range 0.3 – 0.5. Type I gratings have a relatively low thermal stability and degrade noticeably already at temperatures 200 – 300 °C [101]. Nevertheless, such gratings are most often used in practice because they can be comparatively simply written in many fibres. It is assumed that gratings of this type are produced due to the UV radiation-induced transformation of defect centres of a germanosilicate glass resulting in the densification of the glass network. The modification of defect centres, which is accompanied by variations in the parameters of visible and UV absorption bands, and according to the Kramers – Kronig relation, by variations in the refractive index [110], is assigned sometimes to the independent, so-called type 0 photosensitivity. In this case, the type I photosensitivity is related to the densification of the glass network as a whole [116]. At the same time, it seems that these processes proceed simultaneously and, strictly speaking, cannot be separated from each other.

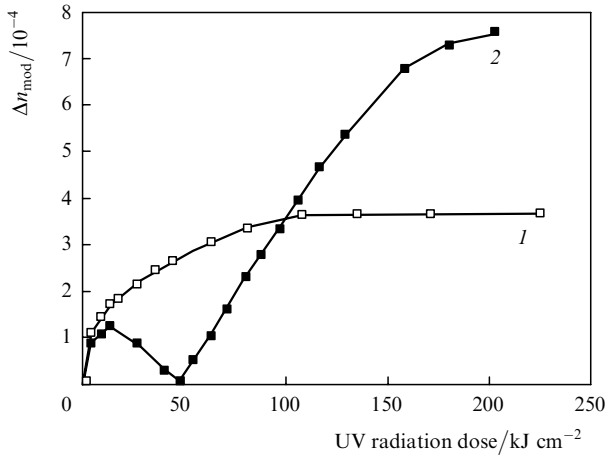

Figure 11. Dependences of the modulation amplitude of the induced refractive index for FBGs written in fibres with the molar concentration of GeO_2 equal to 12 % (*1*) and 35 % (*2*).

Type IIa gratings. During FBG writing in fibres with a high molar concentration of GeO_2 (above 20 %), the modulation amplitude of the induced refractive index (reflectance) in the first diffraction order of the grating first increases, then decreases almost to zero, and then increases again, tending to saturation [curve (*2*) in Fig. 11]. Analysis of the reflectance dynamics in the second diffraction order of the grating and the shift of the resonance wavelength during grating writing suggests that the induced refractive index becomes negative in the maxima of the interference pattern of UV radiation at the second stage of the increase in the reflectance. The effect of a decrease in the induced refractive index upon UV irradiation is called the type IIa photosensitivity, and gratings written in the region of the second rise in the reflectance are called type IIa gratings [117].

At present it is well known that type IIa gratings are closely connected with a change in the elastic stresses in the germanosilicate glass network caused by UV radiation. This is demonstrated, for example, by the fact that the type IIa grating is produced much faster if a tensile stress is applied to a fibre during FBG writing [118]. Type IIa gratings are not formed in bulky samples where gratings are written in a thin layer near the free surface of a sample and, therefore, the structure and value of elastic stresses can be different [119]. It was shown recently [120, 121] that the formation of type IIa gratings is accompanied by a noticeable relaxation of stresses in the fibre core, which causes, in the opinion of the authors, the dilation of the silica glass network.

Note that type IIa gratings are not formed after the low-temperature hydrogen loading. They can be produced only after the out-diffusion of molecular hydrogen from the glass network [122].

Type II gratings. The propagation constant of the fundamental mode of an optical fibre can be strongly changed by irradiating the fibre only by a single pulse from an excimer laser with an energy density of $\sim$1 J cm^{-2}. Irradiation by such a high-power pulse causes an intense heating of the fibre core, which is accompanied by a partial melting of a cladding in contact with the core [123]. Gratings written in such a regime are called type II or IIb gratings. A disadvantage of type II gratings is the complexity of their writing control, especially taking into account that the pulse energy of an excimer laser is, as a rule, not stable from pulse

to pulse. In addition, the asymmetry of induced variations in the glass core properties results in the efficient excitation of cladding modes, which is accompanied by considerable radiation losses to the blue from the main resonance [123]. Note also that irradiation of fibres by such high optical power densities ($\sim 10^8$ W cm^{-2}) causes in some cases a partial damage of the fibre surface, which drastically reduces its mechanical strength. These circumstances prevent wide applications of type II gratings in practice.

Gratings in hydrogen-loaded fibres. It seems that gratings produced in hydrogen-loaded fibres possess an independent type of photosensitivity. Upon exposure to UV radiation, molecular hydrogen enters into the germanosilicate glass network, breaking regular bonds and modifying structural defects. This process is accompanied by the formation of the structural groups Si–OH, Ge–OH, Ge–H, and H_2O [124, 125].

The dose dependence for gratings written in hydrogen-loaded fibres with a low concentration of germanium resembles a power dependence observed for type I gratings; however, the absolute value of the induced refractive index is an order of magnitude higher.

Type Ia gratings. As shown in papers [126, 127], in hydrogen-loaded fibres co-doped with germanium and boron, one more type of photosensitivity appears, which is characterised by the complex dynamics of the reflectance and resonance wavelength. As in type IIa gratings, the increase in the reflectance with increasing the UV radiation dose is followed by its decrease and subsequent increase. At the same time, unlike type IIa photosensitivity, as the UV radiation dose is increased, the resonance wavelength strongly shifts to the blue (by 15–20 nm), which corresponds to the change of the average refractive index in the fibre core by $\sim 2\times 10^{-2}$. Note that the modulation amplitude of the refractive index induced in the grating is two orders of magnitude lower than this value. The authors called gratings with this type of photosensitivity type Ia gratings. An interesting feature of the latter is a lower (by 30 %) thermal sensitivity compared to type I and IIa gratings.

9. Thermal stability of UV induced fibre gratings

A photoinduced fibre grating is erased at high temperatures (300–600 °C), while the photosensitivity in annealed regions of the fibre recovers to its initial value [128]. The study of the thermal stability of the induced refractive index allows one to calculate the spectral characteristics of gratings and the dynamics of their variations during a prolong use of photoinduced structures under different conditions. The latter circumstance is rather important for practical applications of gratings, especially when they are subjected to periodic or constant heating, in particular, in systems for measuring high temperatures.

It was shown in a number of papers that the thermal stability of gratings depends on many factors such as the fibre type [129], method of its processing [101], grating type [130, 131], irradiation dose [132], etc. In addition, it was found that thermal action can result in the formation of gratings of a new type, the so-called 'chemical gratings' [133, 134].

The temperature annealing of the induced refractive index is often described by the approach developed in [135]. It is assumed that changes produced in the glass network by UV radiation have some distribution of the density of potential barriers of the reverse transition. These changes usually imply the transformation of individual defect centres or switching of bonds in the regular glass network, resulting in the formation of thermodynamically nonequilibrium configurations, which should overcome a certain energy barrier E to return to the initial equilibrium state. The population distribution of photoinduced configurations is described by the function $g(E)$. A variation in the energy-barrier height [the width of the function $g(E)$] caused by different local surroundings of these configurations in the glass network is rather large (~ 1 eV). Obviously, the higher is the barrier, the better is the thermal stability of a photoinduced state and a related change in the refractive index of the glass.

The degree of depopulation of photoinduced states depends on temperature T and time t during which the glass is kept at this temperature. To take into account the entire thermal prehistory of a sample, it is convenient to introduce the boundary or demarcation energy E_d, which is described by the expression [135]

$$E_d = kT\ln(v_0 t), \tag{8}$$

where k is the Boltzmann constant; v_0 is the frequency factor, which is of the order of the vibrational frequency 10^{13} Hz of the glass network. The demarcation energy represents in this case a boundary energy level dividing annealed and non-annealed states. The sharpness of the boundary dividing these states is of the order of kT (in the temperature range under study, this is less than 0.1 eV), which is small compared to the width of the distribution $g(E)$.

The knowledge of the distribution $g(E)$ allows us to calculate the degree of decomposition of the induced refractive index for arbitrary annealing of the fibre if the current value of E_d is known. Thus, to describe completely the erasure of the photoinduced refractive index, it is necessary to know $g(E)$ and v_0. These quantities can be determined by constructing the so-called base curve. By differentiating this curve with respect to E_d, the function $g(E)$ can be found [135]. The base curve is the annealing function of the induced refractive index plotted as a function of the demarcation energy and can be obtained by using different annealing regimes.

The thermal stability of gratings is studied by subjecting one or several identical gratings to a certain thermal action and then recording variations in their spectral properties. As a rule, the methods of isothermal or isochronous annealing are used [136] and also the method of linear heating with different rates [137, 138]. The latter approach seems to be the most convenient for obtaining quantitative characteristics of the thermally induced erasure of the induced refractive index. It allows one to determine the required values for a relatively short time with a high accuracy, by having annealed two–three identical gratings.

Figure 12 shows the dependences of the modulation amplitude of the induced refractive index normalised to the initial modulation amplitude at 25 °C which were obtained for the linear annealing of the FBG at a heating rate of 0.25 °C s^{-1} for different types of photoinduced gratings. One can see that the grating written in the hydrogen-loaded fibre has the lowest thermal stability at relatively low

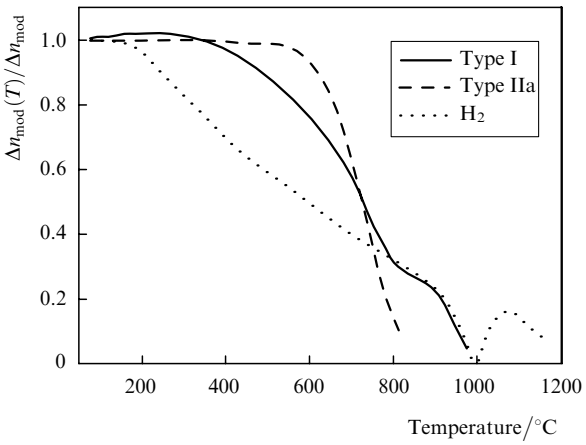

Figure 12. Annealing curves of the induced refractive index in the linear heating regime at a rate of 0.25 °C s^{-1} for FBGs of different types.

temperatures (below 800 °C). At the same time, the refractive index induced in gratings of this type is preserved up to 1000 °C and, moreover, after a complete thermal erasure, the grating appears again at temperatures above 1000 °C. The grating of a new type produced in this way is called 'chemical' because it is produced due to the diffusion of hydrogen-containing groups, which efficiently occurs at such high temperatures [133, 139].

The characteristic feature of type I gratings is the presence of the reverse change in the induced refractive index [140] in the temperature range 100 – 300 °C (see Fig. 12) and a rather complicate behaviour of the annealing curve, which has several parts with different slopes [132]. At moderate temperatures (below 700 °C), the thermal stability of type I gratings is better than that of hydrogen-loaded gratings. At the same time, the most stable at these temperatures are type IIa gratings, which do not change their parameters up to 600 °C and then are rapidly annealed in the temperature range from 600 to 800 °C.

10. Applications of fibre Bragg gratings

As mentioned above, photoinduced fibre gratings are widely used in various devices in fibre optics. First of all, they are employed as spectrally selective elements in fibreoptic communication systems [141], in fibre lasers and amplifiers of different types [142], and systems for measuring physical quantities [30].

Bragg and long-period gratings in fibreoptic communication systems. A permanently growing need to increase the data transfer rate stimulated by the development of telecommunication devices, the increase in information flows, the expansion of global information systems, data bases, and the number of users resulted in the development of fibreoptic communication links employing wave-division multiplexing (WDM). At present standard dense wavelength-division multiplexing (DWDM) communication links are already developed in which the adjacent frequency channels are separated by 50 GHz (about 0.4 nm). The data transfer rate over a channel in experimental communication links exceeds 40 Gbit s^{-1} and a total number of channels achieve 200. A total data transfer rate in such a communication link can exceed 8 Tbit s^{-1}.

It is obvious that such communication links should have input – output devices for individual spectral channels,

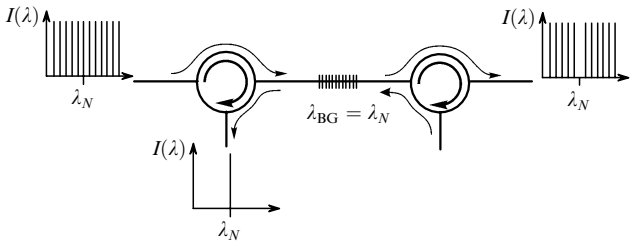

Figure 13. Optical scheme of the input – output device for a specified spectral channel in a fibreoptic communication link.

which can be realised based on FBGs [143]. Figure 13 shows one of the possible schemes of such an input – output selector for an optical channel with the wavelength λ_N based on a highly reflecting FBG and two optical circulators.

In this case, the application of a FBG is limited by the presence of side maxima in the grating spectrum (see Fig. 3) and by optical losses caused by excitation of cladding modes in the grating. As shown above, the side maxima can be suppressed by using the FBG apodization. Some methods were also proposed to suppress resonance excitation of cladding modes [144, 145], which reduced these losses below 0.1 dB.

One of the factors restricting the bit rate in modern communication links is the chromatic dispersion of fibres, which causes broadening and even overlap of laser pulses carrying information. The group-velocity dispersion in standard fibres at a wavelength of 1.55 μm is about 17 ps nm^{-1} km^{-1}, so that, despite low losses in standard fibres (~0.2 dB km^{-1}), the data transfer distance for the 40-Gbit s^{-1} transmission does not exceed 10 km. To increase this distance in operating fibreoptic communication links, it is necessary to compensate their dispersion.

This can be done by means of a compact fibre element, namely, a FBG with a variable period (chirped FBG). Such a grating can introduce a certain time delay between the spectral components of a pulse (Fig. 14), recovering in this way the initial pulse shape [17]. To compensate for dispersion, as a rule, long gratings are required, which are written through a phase mask. At present high-quality gratings of length above 1 m are already available [146]. Dispersion above 1000 ps nm^{-1} achieved in chirped gratings [147] provides the compensation of the broadening of pulses in a 50-km standard fibreoptic communication link at a wavelength of 1.55 μm.

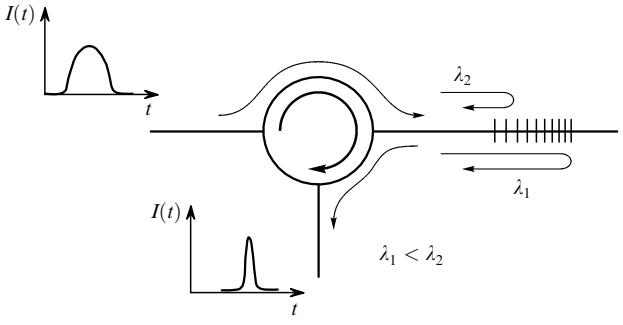

Figure 14. Optical scheme of a dispersion compensator based on a chirped FBG.

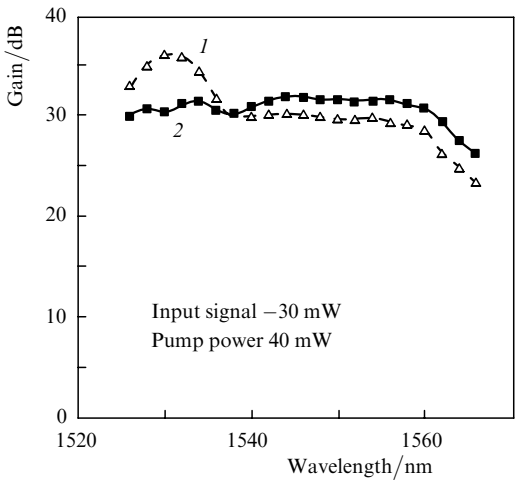

Figure 15. Gain spectra of an erbium-doped fibre amplifier: (*1*) the initial gain spectrum and (*2*) the gain spectrum flattened by using a LPFG [54].

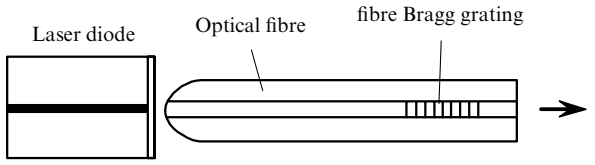

Figure 16. Scheme for stabilisation of semiconductor lasers by means of a FBG.

To transfer information over large distances, it is necessary, along with compensation for the dispersion broadening of pulses, to amplify the optical signal. For this purpose, as a rule, 1.55-μm erbium-doped fibre amplifiers are placed in the communication link through each 50 – 100 km. It is clear that to amplify simultaneously several parallel optical channels, the gain in the spectral range used should be almost constant. As a rule, its variations should not exceed a few tenths of decibel. Unfortunately, the spectral variations of the gain of erbium amplifiers are much greater, which is determined by many factors such as the concentration of erbium ions, their local environment, the wavelength and pump intensity of the amplifier, the active fibre length, etc. The use of fibre gratings makes it possible to modify the gain spectrum by smoothing it or to correct undesirable spectral distortions produced after the signal amplification. A detailed review of applications of fibre gratings for this purpose is presented in [148]. Note only that the gain spectrum can be flattened by using FBGs with fringes perpendicular [149] and tilted [150] to the fibre axis and also LPFGs [54].

Figure 15 illustrates the results of one of the first papers where a uniform LPFG was used to flatten the gain spectrum of an erbium amplifier [54]. The nonuniformity of the gain curve less than 1 dB was achieved for the gain above 30 dB within the spectral band of width 35 nm. The nonuniformity of the gain obtained at present by means of spectral filters is better than 0.1 dB within the same spectral band [148].

FBGs in schemes of diode and fibre lasers. FBGs have found a number of important applications in semiconductor and fibre lasers. The use of gratings allows the flexible tuning of the laser wavelength within the gain band of the active medium of the laser, provides a stable lasing and a decrease in the laser linewidth in some cases, etc. [142].

Figure 16 shows one of the possible schemes of using a FBG as the external resonator of a diode laser. Radiation from a diode laser is coupled to the fibre core by means of a lens formed at the fibre end. The Bragg grating written in the fibre provides feedback at the resonance wavelength λ_{BG}. In particular, the FBG can play the role of a mirror of the external resonator to provide lasing at a single eigenmode of the laser diode, whose wavelength lies within the reflection band of the grating (Fig. 17). To exclude the influence of the own laser resonator, an AR coating is deposited on its output end facing the fibre.

Depending on the grating parameters and the distance between the grating and laser crystal, it is possible to obtain single-frequency or multifrequency lasing [142]. Because the temperature sensitivity of λ_{BG} is approximately an order of magnitude lower than that of the diode laser wavelength, such a configuration allows one to avoid the temperature stabilisation of a laser diode itself in some applications. The above-described scheme for stabilising radiation of semiconductor lasers is used for the development of single-mode pump lasers and light sources in WDM communication systems (as an alternative to distributed-feedback lasers).

FBGs are widely used to form cavities of fibre lasers based on fibres doped with rare-earth ions such as erbium, neodymium, ytterbium, thulium, and holmium. In this case, gratings can be written directly in the active fibre.

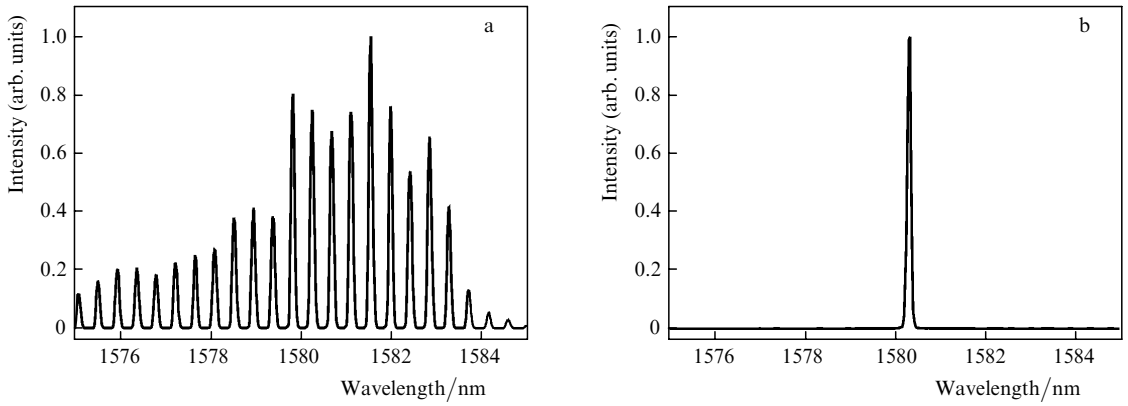

Figure 17. Emission spectra of a diode laser without an external mirror (a) and with a FBG external mirror (b).

Narrowband single-mode fibre lasers with a relatively low output power ($\sim$10 mW) are used in laser spectroscopy, sensors of physical quantities, etc. The lasers of this type include a laser with a comparatively short resonator (a few centimetres) formed by two uniform FBGs [151] and a laser based on a phase-shifted FBG [152].

In the last years high-power double-clad fibre lasers have been actively developed. A great progress in this direction has been achieved first of all due to the development of high-power and reliable semiconductor pump lasers and high-quality double-clad fibres.

The typical structure of a double-clad fibre is shown in Fig. 18. The fibre consists of three layers: single-mode core (*1*) co-doped with a rare-earth ion and impurities forming the refractive index profile, inner silica cladding (*2*), and outer polymer cladding (*3*) with the refractive index lower than that of silica. The inner silica cladding has a typical transverse size of 0.1 – 1 mm, which provides the coupling of pump radiation from semiconductor sources with output powers of a few tens of watts. The pump radiation propagating in the silica cladding is absorbed by active rare-earth ions producing luminescence, which, in the presence of a resonator formed by FBG (*4*), develops to lasing localised in the fibre core of diameter 5 – 10 μm. To provide the more efficient absorption of pump radiation, the silica cladding can have a rectangular or *D*-shaped cross section [153].

Typical characteristics of a double-clad ytterbium-doped fibre laser are illustrated in Fig. 19. Figure 19a shows the luminescence spectrum of the fibre and the laser emission spectrum appearing in the fibre combined with a pair of matched gratings with the resonance wavelength 1103 nm. In this case, a highly reflecting FBG ($R > 99\,\%$) had a spectral width of 0.7 nm, while the spectral width of the output FBG ($R \approx 10\,\%$) was 0.3 nm. Due to their broad luminescence band, ytterbium-doped fibres provide lasing in a broad spectral range from 1050 to 1150 nm with the slope efficiency 50 % – 80 %. Figure 19b shows the dependences of the output laser power on the pump power at 978 nm for different lasing wavelengths [154]. One can see, in particular, that the lasing efficiency decreases away from the luminescence maximum (1.08 – 1.09 μm), remaining, however, at a level of 30 % even at a wavelength of 1148 nm.

Double-clad fibre lasers emitting $\sim$1 kW are already available at present [155]. They are used for laser machining of various materials and also for pumping Raman fibre lasers [156].

Raman fibre lasers emit high-power ($P > 1$ W) cw radiation in a broad spectral range from 1.1 to 2.2 μm [157]. Both standard and special fibres are used for the development of efficient Raman fibre lasers. Although the Raman gain in a glass is comparatively low ($g_R \sim 10^{-13}$ m W^{-1}), efficient lasers can be developed due to low losses, a large interaction length, and a high pump power density ($\sim$1 GW cm^{-2}). The maximum of the Raman band in germanosilicate fibres is located at 440 – 460 cm^{-1}, whereas a phosphosilicate glass fibre has another intense band at $\sim$1330 cm^{-1} [158]. The presence of the latter enables the reduction of the number of cascade Raman conversions by a factor of three to obtain the required output emission wavelength. For example, to obtain lasing at 1480 nm (the pump wavelength of erbium amplifiers) upon pumping by an ytterbium-doped fibre laser in phosphosilicate fibres, it is sufficient to use two Raman conversion cascades, whereas in the case of germanosilicate fibres, 5 – 6 cascades are required [158, 159].

Figure 20 shows the scheme of a two-cascade Raman laser based on a phosphosilicate fibre. In this laser, the 1.06-μm radiation from an ytterbium-doped fibre laser is converted to the 1.48-μm radiation by using two subsequent Raman conversions [159]. To provide the efficient Raman conversion, two embedded resonators were used (at 1.24 and 1.48 μm) formed by FBGs with the corresponding resonance wavelengths. The more efficient utilisation of pump radiation was ensured by using a FBG with the 100 % reflectance at 1.06 μm at the Raman laser output.

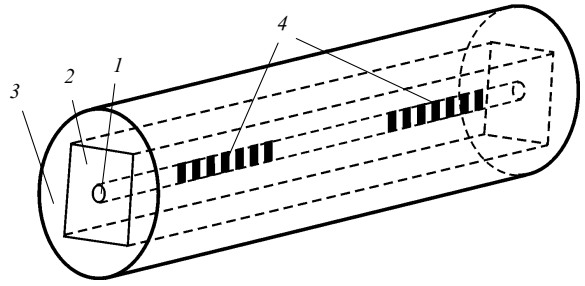

Figure 18. Structure of a double-clad fibre laser: (*1*) core; (*2*) silica glass cladding; (*3*) polymer cladding; (4) FBG.

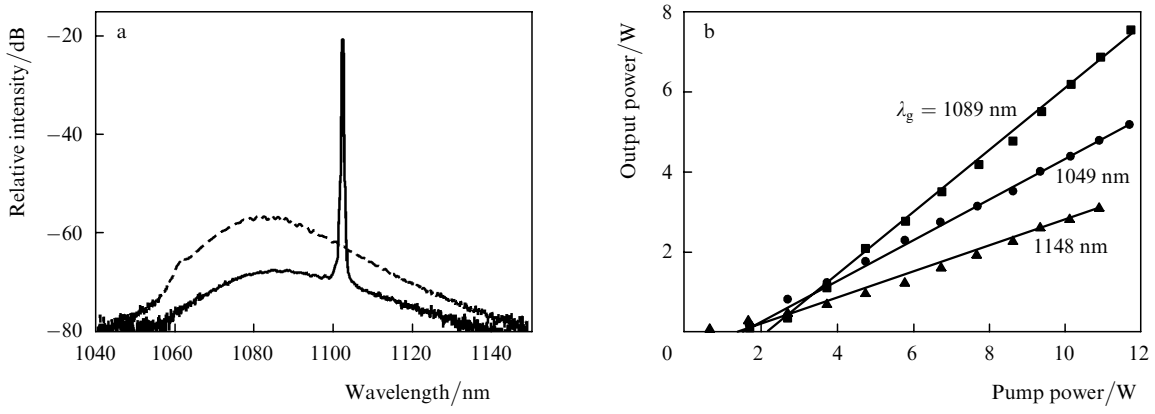

Figure 19. Characteristics of a cladding-pumped ytterbium-doped fibre laser: the luminescence (dashed curve) and lasing (solid curve) spectra (a) and dependences of the output power on the pump power for different lasing wavelengths (b).

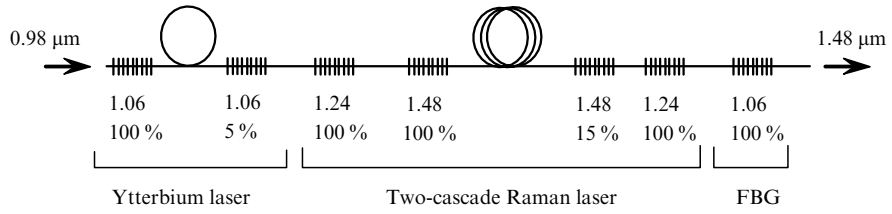

Figure 20. Optical scheme of a two-cascade Raman phosphosilicate fibre laser [159].

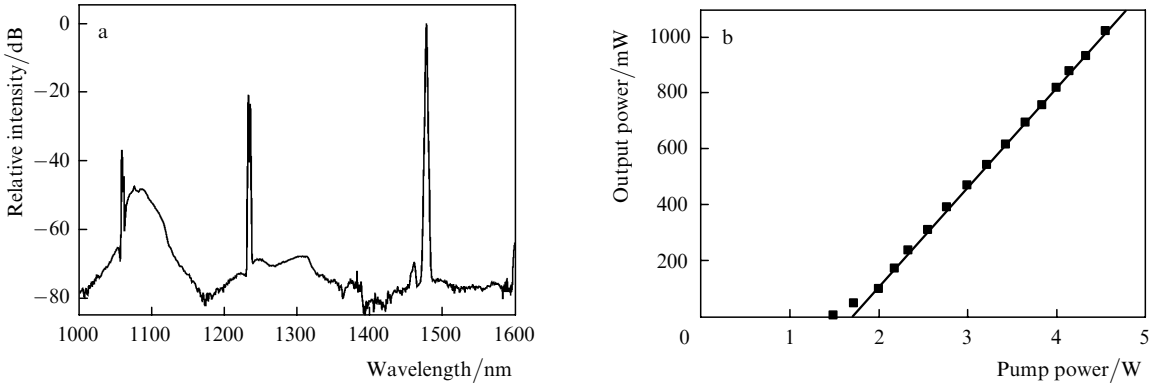

Figure 21. Emission spectrum (a) and dependence of the 1.48-μm emission intensity on the 0.98-μm diode laser pump power (b) for a two-cascade Raman phosphosilicate fibre laser.

Note that the emission spectrum of such a Raman laser contains unabsorbed pump radiation and the ~1.24-μm line corresponding to the intermediate Raman conversion (Fig. 21a). However, the intensity of these lines in the properly optimised laser do not exceed 1 % of the output radiation intensity. Upon pumping by the 5-W, 0.98-μm radiation, the total efficiency of the Raman laser $P_{1.48}/P_{0.98} \approx 22\,\%$ for the slope efficiency ~50 % (Fig. 21b).

FBG sensors of physical quantities. At present FBGs are considered as one of the most promising sensor elements of fibreoptic detectors of physical quantities. They offer a number of advantages such as protection from the action of external electromagnetic fields, high sensitivity, reliability, reproducibility, a wide dynamic range of measurements, the possibility of spectral and spatial multiplexing of sensitive elements located in one or several fibres, a large distance to the place of measurements, a short response time to variations in the measured quantity, high corrosive and radiation resistance, small size and weight, and a number of other advantages.

As mentioned above, the resonance wavelength depends on the fibre temperature and mechanical and tensile or compressive stresses applied to the fibre. FBG sensors used in detectors of physical quantities are based on these properties [3, 30].

The shift of λ_{BG} can be measured by many methods. The most direct method is measuring the transmission (reflection) spectrum of a grating by using a broadband radiation source and a spectrum analyser or a narrowband tunable laser and a photodetector. This method is insensitive to optical losses, which can appear in the optical system during measurements, and provides the high measurement accuracy $\Delta\lambda_{BG}$. However, it requires rather expensive equipment and the time response of this method is limited.

The measurement schemes in which the spectral shift of the resonance wavelength is transformed to a change in the optical signal incident on a photodetector have a faster response. The transformation can be performed, for example, by using an additional spectral filter with an inclined transmission characteristic. In particular, a LPFG can be employed [160]. The slope of the spectral dependence of the filter transmission determines the dynamic range and sensitivity of a fibre sensor.

The methods considered above allow the measurement of physical quantities at the FBG site. However, it is often necessary to find the spatial distribution of the measured quantity. For this purpose, schemes for multiplexing sensor elements were developed, in particular, located in one fibre. These schemes include:

(i) spectral channel multiplexing in which sensor elements are separated in wavelengths;

(ii) the use of optical switches switching one or another of the sensor elements to the measuring system;

(iii) spatiotemporal multiplexing at which the response from each of the gratings is detected at different instants;

(iv) combined schemes including several principles of channel multiplexing listed above.

These schemes for measuring $\Delta\lambda_{BG}$ provide, as a rule, the accuracy of temperature measurement ~0.1 °C and of the relative elongation of the fibre $\sim 10^{-6}$ [30].

Note also that practically important problems of separating the action of temperature and deformations on λ_{BG} and simultaneous measurements of these parameters have been studied in many papers [161].

11. Conclusions

We have shown in our review that photoinduced refractive-index structures are widely used for the development of various, including essentially new elements, devices, and

systems in fibre optics. At present the study of the photosensitivity of silica glasses and silica fibres, the fabrication of fibre gratings of different types with different properties, and applications of these gratings represent an independent and very important direction in fibre optics. The unique spectral and dispersion characteristics of fibre gratings, the permanent development and improvement of the grating production methods, the increasing knowledge of fundamental mechanisms of photosensitivity of silica glasses – all these allow us to assert with confidence that interest in fibre gratings and their applications will increase in the future.

Because it is practically impossible to present even briefly all the experimental and theoretical results accumulated in this field, we restricted ourselves to the description and some generalisation of the most important, in our opinion, results, methods, and approaches existing at present. A more detailed description of the results concerning specific problems can be found in original papers presented in references.

Acknowledgements. This work was supported by the Russian Foundation for Basic Research (Grant No. 04-02-17025) and the Moscow Committee on Science and Technologies (Grant No. 1.2.30, 2004).

References

1. *J. Lightwave Technol.*, **15** (8) (1997).
2. Kashyap R. *Fiber Bragg Gratings* (San Diego, CA: Acad. Press, 1999).
3. Othonos A., Kalli K. *Proc. Fiber Bragg Gratings: Fundamentals and Applications in Telecommunications and Sensing* (Norwood, Mass.: Artech House, 1999).
4. Hill K.O., Fujii Y., Johnson D.C., Kawasaki B.S. *Appl. Phys. Lett.*, **32**, 647 (1978).
5. Lam D.K.W., Garside B.K. *Appl. Opt.*, **20**, 440 (1981).
6. Meltz G., Morey W.W., Glenn W.H. *Opt. Lett.*, **14**, 823 (1989).
7. Kogelnik H. *Theory of Optical Waveguides, in Guided-Wave Optoelectronics*. Ed. by T. Tamir (Berlin – Geidelberg – New York: Springer-Verlag, 1988).
8. Vasiliev S.A., Medvedkov O.I. *Proc. SPIE Int. Soc. Opt. Eng.*, **4083**, 212 (2000).
9. Erdogan T. *J. Opt. Soc. Am. A*, **14**, 1760 (1997).
10. Vasil'ev S.A., Dianov E.M., Kurkov A.S., Medvedkov O.I., Protopopov V.N. *Kvantovaya Elektron.*, **24**, 151 (1997) [*Quantum Electron.*, **27**, 146 (1997)].
11. Shu X., Zhang L., Bennion I. *J. Lightwave Technol.*, **20**, 255 (2002).
12. Bilodeau F., Hill K.O., Malo B., Johnson D.C., Skinner I.M. *Electron. Lett.*, **27**, 682 (1991).
13. Russell P.St.J., Hand D.P. *Electron. Lett.*, **26**, 1846 (1990).
14. Hill K.O., Bilodeau F., Malo B., Johnson D.C. *Electron. Lett.*, **27**, 1548 (1991).
15. Albert J., Hill K.O., Malo B., Thriault S., Bilodeau F., Johnson D.C., Erickson L.E. *Electron. Lett.*, 31, 222 (1995).
16. Erdogan T. *J. Lightwave Technol.*, **15**, 1277 (1998).
17. Williams J.A.R., Bennion I., Sugden K., Doran N.J. *Electron. Lett.*, **30**, 985 (1994).
18. Kashyap R., Mckee P.F., Campbell R.J., Williams D.L. *Electron. Lett.*, **30**, 996 (1994).
19. Zhang L., Sugden K., Williams J.A.R., Bennion I. *Photosensitivity and Quadratic Nonlinearity in Glass Waveguides, Techn. Dig. Series, 22* (Washington, DC: OSA, 1995) SuB11.
20. Loh W.H., Laming R.I., Ellis A.D., Atkinson D. *Proc. Opt. Fiber Commun. Conf.* (Washington, DC: OSA, 1996) PD30.
21. Sugden K., Bennion I., Molony A., Copner N.J. *Electron. Lett.*, **30**, 440 (1994).
22. Hill K.O. et al. *Opt. Lett.*, **19**, 1314 (1994).
23. Kashyap R., McKee P.F., Armes D. *Electron. Lett.*, **30**, 1977 (1994).
24. Canning, J., Sceats M.G. *Electron. Lett.*, **30**, 1344 (1994).
25. Eggleton B.J. et al. *Electron. Lett.*, **30**, 1620 (1994).
26. Ouellette F., Krug P.A., Stephens T., et al. *Electron. Lett.*, **31**, 899 (1995).
27. Othonos A., Lee X., Measures R.M. *Electron. Lett.*, **30**, 1972 (1994).
28. Kashyap R., Wyatt R., McKee P.F. *Electron. Lett.*, **29**, 1025 (1993).
29. Mizunami T., Djambova T.V., Niiho T., Gupta S. *J. Lightwave Technol.*, **18**, 230 (2000).
30. Kersey A.D., Davis M.A., Patrick H.J., LeBlanc M., Koo K.P., Askins C.G., Putnam M.A., Friebele E.J. *J. Lightwave Technol.*, **15**, 1442 (1997).
31. Vengsarkar A.M., Lemaire P.J., Judkins J.B., Bhatia V., Sipe J.E., Erdogan T. *Proc. Opt. Fiber Commun. Conf.* (Washington, DC: OSA, 1995) PD4-2.
32. Vasil'ev S.A., Dianov E.M., Medvedkov O.I., Protopopov V.N., Konstantini D.M., Iocco A., Limberger H.G., Salate R.P. *Kvantovaya Elektron.*, **26**, 65 (1999) [*Quantum Electron.*, **29**, 65 (1999)].
33. Erdogan T., Stegall D. *Proc. Opt. Fiber Commun. Conf.* (Washington, DC: OSA, 1998) ThG5.
34. Dianov E.M., Kurkov A.S., Medvedkov O.I., Vasiliev S.A. *Proc. Eurosensors X* (Leuven, Belgium, 1996) p. 5.1, 128.
35. Bhatia V., Vengsarcar A.M. *Opt. Lett*, **21**, 692 (1996).
36. Bhatia V., Campbell D., Claus R., Vengsarkar A.M. *Opt. Lett.*, **22**, 648 (1997).
37. Lee B.H., Liu Y., Lee S.B., Choi S.S. *Opt. Lett.*, **22**, 1769 (1997).
38. Patrick H.J., Chang C.C., Vohra S.T. *Electron. Lett.*, **34**, 1773 (1998).
39. Rathje J., Svalgaard M., Hubner H., Kristensen M. *Proc. Opt. Fiber Commun. Conf.* (Washington, DC: OSA, 1998) WM49, p. 238.
40. Patrick H.J. *Electron. Lett.*, **36**, 1763 (2000).
41. Vasiliev S.A., Dianov E.M., Varelas D., Limberger H., Salathe R.P. *Opt. Lett.*, **21**, 1830 (1996).
42. Korolev I.G. *Cand. Sci. Dissertation* (Moscow, IOF RAN, 2004).
43. Grubsky V., Skorucak A., Starodubov D.S., Feinberg J. *Proc. Opt. Fiber Commun. Conf.* (Washington, DC: OSA, 1999) FK5, p. 174.
44. Ramachandran S., Wagener J., Espindola R., Strasser T. *Bragg Gratings, Photosensitivity, and Poling in Glass Waveguides, OSA Tech. Dig.* (Washington, DC: OSA, 1999) Paper SaC3, p. 286.
45. Deparis O., Kiyan R., Pottiez O., Blondel M., Korolev I.G., Vasiliev S.A., Dianov E.M. *Opt. Lett.*, **26**, 1239 (2001).
46. Dianov E.M., Vasiliev S.A., Kurkov A.S., Medvedkov O.I., Protopopov V.N. *Proc. Europ. Conf. on Opt. Commun.* (Oslo, 1996) MoB3.6, p. 65.

47. Dianov E.M., Vasil'ev S.A., Medvedkov O.I., Frolov A.A. *Kvantovaya Elektron.*, **24**, 805 (1997) [*Quantum Electron.*, **27**, 785 (1997)].
48. Hill K.O., Malo B., Bilodeau F., Johnson D.C., Albert J. *Appl. Phys. Lett.*, **62**, 1035 (1993).
49. Dyer P.E., Farley R.J., Giedl R. *Opt. Commun.*, **129**, 98 (1996).
50. Byron K.C., Sugden K., Bircheno T., Bennion I. *Electron. Lett.*, **29**, 1659 (1993).
51. Varming P., Jensen J.B., Plougmann N., Kristensen M, Hubner J. *Bragg Gratings, Photosensitivity, and Poling in Glass Waveguides, OSA Tech. Dig.* (Washington, DC: OSA, 2001) BWA5.
52. Dong L. et al. *Electron. Lett.*, **29**, 1577 (1993).
53. Askins C.G. et al. *Opt. Lett.*, **19**, 147 (1994).
54. Dianov E.M., Karpov V.I., Kurkov A.S., Medvedkov O.I., Prokhorov A.M., Protopopov V.N., Vasiliev S.A. *Photosensitivity and Quadratic Nonlinearity in Glass Waveguides, Techn. Dig. Series, 22* (Washington, DC: OSA, 1995) SaB3, p. 14.
55. Dianov E.M., Starodubov D.S., Vasiliev S.A., Frolov A.A., Medvedkov O.I. *Opt. Lett.*, **22**, 221 (1997).
56. Narayanan C., Presby H.M., Vengsarkar A.M. *Proc. Opt. Fiber Commun. Conf.* (Washington, DC: OSA, 1996) ThP3, p. 267.
57. Akiyama M., Nishide K., Shima K., Wada A., Yamauchi R. *Proc. Opt. Fiber Commun. Conf.* (Washington, DC: OSA, 1998) ThG1, p. 276.
58. Enomoto T., Shigehara M., Ishikawa S., Danzuka T., Kanamori H. *Proc. Opt. Fiber Commun. Conf.* (Washington, DC: OSA, 1998) ThG2, p. 277.
59. Karpov V.I., Grekov M.V., Dianov E.M., Golant K.M., Vasiliev S.A., Medvedkov O.I., Khrapko R.R. *Proc. Opt. Fiber Commun. Conf.* (Washington, DC: OSA, 1998) ThG4.
60. Dianov E.M., Karpov V.I., Kurkov A.S., Grekov M.V. *Proc. Europ. Conf. on Opt. Commun.* (Madrid, Spain, 1998) p. 395.
61. Davis D.D., Gaylord T.K., Glytsis E.N., Mettler S.C. *Electron. Lett.*, **34**, 1416 (1998).
62. Dianov E.M., Karpov V.I., Grekov M.V., Golant K.M., Vasiliev S.A., Medvedkov O.I., Khrapko R.R. *Proc. Europ. Conf. on Opt. Commun.* (Edinburg, UK, 1997) p. 53.
63. Godbout N., Daxhelet X., Maurier A., Lacroix S. *Proc. Europ. Conf. on Opt. Commun.* (Madrid, Spain, 1998) p. 397.
64. Kosinski S.G., Vengsarkar A.M. *Proc. Opt. Fiber Commun. Conf.* (Washington, DC: OSA, 1998) ThG3, p. 278.
65. Sohn I., Baek J., Lee N., Kwon H., Song J. *Electron. Lett.*, **38**, 1324 (2002).
66. Ivanov O.V., Wang L.A. *Appl. Opt.*, **42**, 2264 (2003).
67. Kim H.S., Yun S.H., Hwang I.K., Kim B.Y. *Proc. Optoelectron. & Commun. Conf.* (Seoul, Korea, 1997) 9D2-6, p. 226.
68. Diez A., Birks T.A., Reeves W.H., Mangan B.J., Russell P.St.J. *Opt. Lett.*, **25**, 1499 (2000).
69. Kakarantzas G., Birks T.A., Russell P.St.J. *Opt. Lett.*, **27**, 1013 (2002).
70. Lim J.H., Lee K.S., Kim J.C., Lee B.H. *Opt. Lett.*, **29**, 331 (2004).
71. Eggleton B.J., Westbrook P.S., Windeler R.S. *Opt. Lett.*, **24**, 1460 (1999).
72. Fu L.B., Marshall G.D., Bolger J.A., et al. *Electron. Lett.*, **41**, 638 (2005).
73. Neustruev V.B. *J. Phys.: Condens. Matter*, **6**, 6901 (1994).
74. Dianov E.M., Vasil'ev S.A., Starodubov D.S., Frolov A.A., Medvedkov O.I. *Kvantovaya Elektron.*, **24**, 160 (1997) [*Quantum Electron.*, **27**, 155 (1997)].
75. Starodubov D.S., Grubsky V., Feinberg J., Dianov E.M., Semjonov S.L., Guryanov A.N., Vechkanov N.N. *Bragg Gratings, Photosensitivity, and Poling in Glass Waveguides, OSA Tech. Dig.* (Washington, DC: OSA, 1997) PDP1.
76. Albert J., Malo B., Bilodeau F., Johnson D.C., Hill K.O., Hibino Y., Kawachi M. *Opt. Lett.*, **19**, 387 (1994).
77. Herman P.R., Beckley K., Ness S. *Bragg Gratings, Photosensitivity, and Poling in Glass Waveguides, OSA Tech. Dig.* (Washington, DC: OSA, 1997) BME4, p. 159.
78. Mihailov S.J., Smelser C.W., Lu P., Walker R.B., Grobnic D., Ding H., Henderson G., Unruh J. *Opt. Lett.*, **28**, 995 (2003).
79. Dragomir A., Nikogosyan D.N., Zagorulko K.A., Kryukov P.G., Dianov E.M. *Opt. Lett.*, **28**, 2171 (2003).
80. Mihailov S.J., Smelser C.W., Grobnic D., Walker R.B., Lu P., Ding H., Unruh J. *J. Lightwave Technol.*, **22**, 94 (2004).
81. Mihailov S.J., Smelser C.W., Grobnic D., Walker R.B., Ding H., Lu P. *Proc. Opt. Fiber Commun. Conf.* (Washington, DC: OSA, 2005) OFC6.
82. Williams D.L., Ainslie B.J., Armitage J.R., Kashyap R., Campbell R.J. *Proc. Europ. Conf. on Opt. Commun.* (Berlin, Germany, 1992) WeB9-5, p. 425.
83. Dong L., Pinkstone J., Russell P.St.J., Payne D.N. *Proc. Conf. on Lasers and Opto-Electronics, CLEO'94* (Anaheim, CA, USA, 1994) p. 243.
84. Mashinsky V.M., Medvedkov O.I., Neustruev V.B., Dvoyrin V.V., Vasiliev S.A., Dianov E.M., Khopin V.F., Guryanov A.N. *Proc. Europ. Conf. on Opt. Commun.* (Rimini, Italy, 2003) Tu1.7.2.
85. Dianov E.M., Golant K.M., Khrapko R.R., Kurkov A.S., et al. *Electron. Lett.*, **33**, 236 (1997).
86. Dong L., Pinkstone J., Russell P.St.J., Payne D.N. *J. Opt. Soc. Amer. B*, **11**, 2106 (1994).
87. Gruner-Nielsen L., Hubner J. *Proc. Opt. Fiber Commun. Conf.* (Washington, DC: OSA, 1997, WL16, 178).
88. Williams D.L., Ainslie B.J., Armitage J.R., Kashyap R. *Electron. Lett.*, **29**, 45 (1993).
89. Ivanov G.A., Aksenov V.A., Kurkov A.S., Medvedkov A.I., Pershina E.V., Dianov E.M. *Radiotekh. Radioelektron.*, **46**, 1 (2001).
90. Dong L., Cruz J.L., Reekie L., Xu M.G., Payne D.N. *Photosensitivity and Quadratic Nonlinearity in Glass Waveguides, Techn. Dig. Series* (Washington, DC: OSA, 1995) Vol. 22, SuA2, p. 70.
91. Dianov E.M., Golant K.M., Mashunsky V.M., Medvedkov O.I., Nikolin I.V., Sazhin O.D., Vasiliev S.A. *Electron. Lett.*, **33**, 1334 (1997).
92. Dong L., Reekie L., Cruz J.L., Payne D.N. *Proc. Opt. Fiber Commun. Conf.* (Washington, DC: OSA, 1996) TuO2, p. 82.
93. Shen Y., He J., Sun T., Grattan K.T.V. *Opt. Lett.*, **29**, 554 (2004).
94. Canning J., Sceats M.G., Hill P. *Opt. Lett.*, **20**, 2189 (1995).
95. Strasser T.A., White A.E., Yan M.F., Lemaire P.J., Erdogan T. *Proc. Opt. Fiber Commun. Conf.* (Washington, DC: OSA, 1995) p. 159.
96. Gerasimova V.I., Rybaltivskii A.O., Chernov P.V., Mashinskii V.M., Sazhin O.D., Medvedkov O.I., Rybaltovskii A.A., Khrapko R.R. *Kvantovaya Elektron.*, **33**, 90 (2003) [*Quantum Electron.*, **33**, 90 (2003)].

97. Oh K., Westbrook P.S., Atkins R.M., Reyes P., Windeler R.S., Reed W.A., Stockert T.E., Brownlow D., DiGiovanni D. *Opt. Lett.*, **27**, 488 (2002).
98. Bilodeau F., Malo B., Albert A., Johnson D.C., Hill K.O., Hibino Y., Abe M., Kawachi M. *Opt. Lett.*, **18**, 953 (1993).
99. Lemaire P.J., Atkins R.M., Mizrahi V., Reed W.A. *Electron. Lett.*, **29**, 1191 (1993).
100. Lemaire P.J. *Opt. Eng.*, **30**, 780 (1991).
101. Patrick H., Gilbert S.L., Lidgard A., Gallagher M.D. *J. Appl. Phys.*, **78**, 2940 (1995).
102. Malo B., Albert J., Hill K.O., Bilodeau F., Johnson D.C. *Electron. Lett.*, **30**, 442 (1994).
103. Faerch K., Svalgaard M. *Bragg Gratings, Photosensitivity, and Poling in Glass Waveguides, OSA Tech. Dig.* (Washington, DC: OSA, 2003) TuA2, p. 178.
104. Bhakti F., Larrey J., Sansonetti P., Poumellec B. *Bragg Gratings, Photosensitivity, and Poling in Glass Waveguides, OSA Tech. Dig.* (Washington, DC: OSA, 1997) BSuD4, p.55.
105. Araujo F.M., Joanni E., Marques M.B., Okhotnikov O.G. *Appl. Phys. Lett.*, **72**, 3109 (1998).
106. Stone J. *J. Lightwave Technol.*, **5**, 712 (1987).
107. Aslund M., Canning J., Yoffe G. *Opt. Lett.*, **24**, 1826 (1999).
108. Salik E., Starodubov D.S., Grubsky V., Feinberg J. *Proc. Opt. Fiber Commun. Conf.* (Washington, DC: OSA, 2000) TuH4.
109. Hand D.P., Russell P.St.J. *Opt. Lett.*, **15**, 102 (1990).
110. Dong L., Archambault J.L., Reekie L., Russell P.S.J., Payne D.N. *Appl. Opt.*, **34**, 3436 (1995).
111. Poumellec B., Guenot P., Riant I., Sansonetti P., Niay P., Bernage P., Bayon J.F. *Opt. Mater.*, **4**, 441 (1995).
112. Riant I., Borne S., Sansonetti P., Poumellec B. *Photosensitivity and Quadratic Nonlinearity in Glass Waveguides, Techn. Dig. Series* (Washington, DC: OSA, 1995) Vol. 22, SaD3, p. 52.
113. Dianov E.M., Plotnichenko V.G., Koltashev V.V., Pyrkov Yu.N., Ky N.H., Limberger H.G., Salathe R.P. *Opt. Lett.*, **22**, 1754 (1997).
114. Fonjallaz P.Y., Limberger H.G., Salathe R.P., Cochet F., Leuenberger B. *Opt. Lett.*, **20**, 1346 (1995).
115. Patrick H., Gilbert S.L. *Opt. Lett.*, **18**, 1484 (1993).
116. Poumellec B., Niay P., Douay M., Bayon J.F. *J. Phys. D: Appl. Phys.*, **29**, 1842 (1996).
117. Xie W.X., Douay M., Bernage P., Niay P., Bayon J.F., Georges T. *Opt. Commun.*, **101**, 85 (1993).
118. Taunay T., Niay P., Bernage P., Douay M., Xie W.X., Pureur D., Cordier P., Bayon J.F., Poignant H., Delevaque E., Poumellec B. *J. Phys. D: Appl. Phys.*, **30**, 40 (1997).
119. Xie W.X., Niay P., Bernage P., Douay M., Taunay T., Bayon J.F., Delevaque E., Monerie M. *Opt. Commun.*, **124**, 295 (1996).
120. Canning J., Aslund M. *Opt. Lett.*, **24**, 463 (1999).
121. Ky N.H., Limberger H.G., Salathe R.P., Cochet F., Dong L. *Opt. Commun.*, **225**, 313 (2003).
122. Poignant H., Bayon J.F., Delevaque E., Monerie M., Mellot J.L., Grot D., Niay P., Bemage P., Douay M. *IEE Colloquium on Optical Fibre Gratings* (IEE Digest 6 1997/037, 1997) p. 2/1.
123. Archambault J-L., Reekie L., Russell P.St.J. *Electron. Lett.*, **29**, 28 (1993).
124. Cordier P., Dalle C., Depecker C., Bernage P., Douay M., Niay P., Bayon J.-F., Dong L. *J. Non-Cryst. Sol.*, **224**, 277 (1998).
125. Dianov E.M., Skolov V.O., Sulimov V.B. *Volokon.-opt. tekhnol, mater. i ustr.*, **2**, 53 (1999).
126. Liu Y., Shu X., Floreani F., Zhang L., Williams J.A.R., Bennion I. *Proc. Summer Schools on Photosensitivity in Optical Wavequides and Glasses* (S.-Petersburg, 2002, WA4) p. 40.
127. Liu Y., Williams J.A.R., Zhang L., Bennion I. *Opt. Lett.*, **27**, 586 (2002).
128. Atkins R.M., Mizrahi V. *Electron. Lett.*, **28**, 1743 (1992).
129. Baker S.R., Rourke H.N., Baker V., Goodchild D. *J. Lightwave Technol.*, **15**, 1470 (1997).
130. Dong L., Liu W.F. *Appl. Opt.*, **36**, 8222 (1997).
131. Archambault J.-L., Reekie L., Russell P.St.J. *Electron. Lett.*, **29**, 453 (1993).
132. Vasiliev S.A., Medvedkov O.I., Bozhkov A.S., Dianov E.M. *Bragg Gratings, Photosensitivity, and Poling in Glass Waveguides, OSA Tech. Dig.* (Washington, DC: OSA, 2003) MD31, p. 145.
133. Fokine M. *Opt. Lett.*, **27**, 1016 (2002).
134. Fokine M. *J. Opt. Soc. Am. B*, **19**, 1759 (2002).
135. Erdogan T., Mizrahi V., Lemaire P.J., Monroe D. *J. Appl. Phys.*, **76**, 73 (1994).
136. Razafimahatratra D., Niay P., Douay M., Poumellec B., Riant I. *Appl. Opt.*, **39**, 1924 (2000).
137. Rathje J., Kristensen M., Pedersen J.E. *J. Appl. Phys.*, **88**, 1050 (2000).
138. Bozhkov A.S., Vasil'ev S.A., Medvedkov O.I., Grekov M.V., Korolev I.G. *Prob. Tekh. Eksp.*, **48**, 491 (2005).
139. Grubsky V., Starodubov D., Morey W.W. *Bragg Gratings, Photosensitivity, and Poling in Glass Waveguides, OSA Tech. Dig.* (Washington, DC: OSA, 2003) MB5, p. 33.
140. Hidayat A., Wang Q., Niay P., Douay M., Poumellec B., Kherbouche F., Riant I. *Appl. Opt.*, **40**, 2632 (2001).
141. Giles C.R. *J. Lightwave Technol.*, **15**, 1391 (1997).
142. Archambbault J.-L., Grubb S.G. *J. Lightwave Technol.*, **15**, 1378 (1997).
143. Bilodeau F., Johnson D.C., Theriault S., Malo B., Albert J., Hill K.O. *IEEE Photon. Technol. Lett.*, **7**, 388 (1995).
144. Dong L., Reekie L., Cruz J.L., Caplen J.E., Sandro J.P., Payne D.N. *IEEE Photon. Technol. Lett.*, **9**, 64 (1997).
145. Delevaque E., Boj S., Bayon J.-F., Poignant H., Le Mellot J., Monerie M. *Proc. Opt. Fiber Commun. Conf.* (Washington, DC: OSA, 1995) PD5.
146. Kashyap R., Froehlich H-G., Swanton A., Armes D.J. *Electron. Lett.*, **32**, 1807 (1996).
147. Hill K.O., Theriault S., Malo B., Belodeau F., Kitagawa T., Johnson D.C., Albert J., Takiguchi T., Takaoka T., Hagimoto K. *Electron. Lett.*, **30**, 1755 (1994).
148. Riant I. *Opt. Fiber Techn.*, **8**, 171 (2002).
149. Rochette M., Guy M., LaRochelle S., Lauzon J., Trepanier F. *IEEE Photon. Technol. Lett.*, **11**, 536 (1999).
150. Kashyap R., Wyatt R., Campbell R.J. *Electron. Lett.*, **29**, 154 (1993).
151. Ball G.A., Glenn W.H. *J. Lightwave Technol.*, **10**, 1338 (1992).
152. Loh W.H., Dong L., Caplen J.E. *Appl. Phys. Lett.*, **69**, 2151 (1996).
153. Liu A., Ueda K. *Opt. Commun.*, **132**, 511 (1996).
154. Kurkov A.S., Dianov E.M., Paramonov V.M., Gur'yanov A.N., Laptev A.Yu., Khopin V.F., Umnikov A.A., Vechkanov N.I., Medvedkov O.I., Vasil'ev S.A., Bubnov M.M., Egorova O.N., Semenov S.L., Pershina E.V. *Kvantovaya Elektron.*, **30**, 791 (2000) [*Quantum Electron.*, **30**, 791 (2000)].

155. Jeong Y., Sahu J.K., Baek S., Alegria C., Codemard C.A., Soh D.B.S., Philippov V., Williams R.B., Furusawa K., Richardson D.J., Payne D.N., Nilsson J. *Proc. Annual Meeting of the IEEE Lasers and Electro-Optics Society* (Tucson, Arisona, 2003) ThD1.
156. Grubb G.S. et al. *Proc. Opt. Amplifiers and Their Applications* (Washington, DC: OSA, 1995) SaA4.
157. Dianov E.M., Bufetov I.A., Mashinskii V.M., Shubin A.V., Medvedkov O.I., Rakitin A.E., Mel'kumov M.A., Khopin V.F., Gur'yanov A.N. *Kvantovaya Elektron.*, **35**, 435 (2005) [*Quantum Electron.*, **35** 435 (2005)].
158. Dianov E.M., Grekov M.V., Bufetov I.A., Vasiliev S.A., Medvedkov O.I., Plotnichenko V.G., Koltashev V.V., Belov A.V., Bubnov M.M., Semyonov S.L., Prokhorov A.M. *Electron. Lett.*, **33**, 1542 (1997).
159. Karpov V.I., Dianov E.M., Paramonov V.M., Medvedkov O.I., Bubnov M.M., Semyonov S.L., Vasiliev S.A., Protopopov V.N., Egorova O.N., Hopin V.F., Guryanov A.N., Bachynski M.P., Clements W.R.L. *Opt. Lett.*, **24**, 887 (1999).
160. Protopopov V.N., Karpov V.I., Medvedkov O.I., Vasiliev S.A., Grekov M.V., Dianov E.M., Palto S.P. *Proc. SPIE Int. Soc. Opt. Eng.*, **4083**, 224 (2000).
161. Jones J.D.C. *Proc. Optical Fibre Sensor Conf.* (Williamsburg, VA, USA, 1997) p. 36.